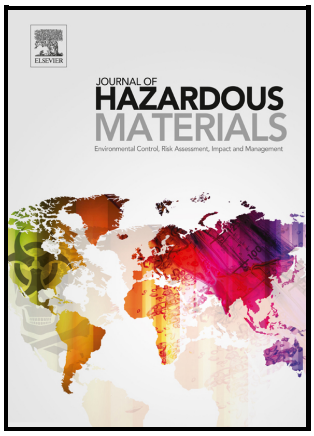

Effect of micro- and nanoplastic particles on human macrophages

Maike Y Adler, Insaf Issoual, Michael Rückert, Lisa Deloch, Carola Meier, Thomas Tschernig, Christoph Alexiou, Felix Pfister, Anja FRM Ramsperger, Christian Laforsch, Udo Gaipl, Katharina Jüngert, Friedrich Paulsen

PII: S0304-3894(24)00832-X

DOI: https://doi.org/10.1016/j.jhazmat.2024.134253

Reference: HAZMAT134253

To appear in: *Journal of Hazardous Materials*

Received date: 26 January 2024
Revised date: 27 March 2024
Accepted date: 8 April 2024

Please cite this article as: Maike Y Adler, Insaf Issoual, Michael Rückert, Lisa Deloch, Carola Meier, Thomas Tschernig, Christoph Alexiou, Felix Pfister, Anja FRM Ramsperger, Christian Laforsch, Udo Gaipl, Katharina Jüngert and Friedrich Paulsen, Effect of micro- and nanoplastic particles on human macrophages, *Journal of Hazardous Materials,* (2024) doi:https://doi.org/10.1016/j.jhazmat.2024.134253

Effect of micro- and nanoplastic particles on human macrophages

Maike Y Adler[1], Insaf Issoual[1,2], Michael Rückert[3,4,5], Lisa Deloch[3,4,5], Carola Meier[6], Thomas Tschernig[6], Christoph Alexiou[7], Felix Pfister[7], Anja FRM Ramsperger[8], Christian Laforsch[8], Udo Gaipl[3,4,5], Katharina Jüngert[1*], Friedrich Paulsen[1*]

1 Functional and Clinical Anatomy, Friedrich-Alexander-Universität Erlangen-Nürnberg, Germany

2 Chair of Machine Learning and Data Analytics, Friedrich-Alexander-Universität Erlangen-Nürnberg, Germany

3 Translational Radiobiology, Department of Radiation Oncology, Universitätsklinikum Erlangen, Friedrich-Alexander-Universität Erlangen-Nürnberg, Erlangen, Germany.

4 Department of Radiation Oncology, Universitätsklinikum Erlangen, Friedrich-Alexander-Universität Erlangen-Nürnberg, Erlangen, Germany.

5 Comprehensive Cancer Center Erlangen-EMN, Erlangen, Germany

6 Institute of Anatomy and Cell Biology, Saarland University, Homburg/Saar, Germany

7 Department of Otorhinolaryngology, Head and Neck Surgery, Section of Experimental Oncology and Nanomedicine (SEON), Else Kröner-Fresenius-Stiftung Professorship, Universitätsklinikum Erlangen, Erlangen, Germany

8 Animal Ecology I and Bay CEER, University of Bayreuth, Bayreuth, Germany

*Both authors contributed equally

Abstract

Micro- and nanoplastics (MNPs)[1] are ubiquitous in the environment, resulting in the uptake of MNPs by a variety of organisms, including humans, leading to particle-cell interaction. Human macrophages derived from THP-1 cell lines take up Polystyrene (PS)[2], a widespread plastic. The question therefore arises whether primary human macrophages also take up PS micro- and nanobeads (MNBs)[3] and how they react to this stimulation. Major aim of this study is to visualize this uptake and to validate the isolation of macrophages from peripheral blood mononuclear cells (PBMCs)[4] to assess the impact of MNPs on human macrophages. Uptake of macrophages from THP-1 cell lines and PBMCs was examined by transmission electron microscopy (TEM)[5], scanning electron microscopy and live cell imaging. In addition, the reaction of the macrophages was analyzed in terms of metabolic activity, cytotoxicity, production of reactive oxygen species (ROS)[6] and macrophage polarization. This study is the first to visualize PS MNBs in primary human cells using TEM and live cell imaging. Metabolic activity was size- and concentration-dependent, necrosis and ROS were increased. The

[1] MNPs – micro- and nanoplastics

[2] PS - Polystyrene

[3] MNBs – micro- and nanobeads

[4] PBMCs – peripheral blood mononuclear cells

[5] TEM – transmission electron microscopy

[6] ROS – reactive oxygen species

methods demonstrated in this study outline an approach to assess the influence of MNP exposure on human macrophages and help investigating the consequences of worldwide plastic pollution.

Environmental implication

Polystyrene micro- and nanoplastics are among the plastic particles which can be found worldwide in different ecosystems (1). Because of their size, they can enter the food chain and accumulate in a large variety of organisms (2). Previous studies already showed a cytotoxic effect on murine macrophages and human dTHP-1 (3, 4). However more research is needed to assess the impact of this distribution on humans. Studying the consequences of human plastic exposure and potential health risks using a human macrophage model, supports the process of political decision-making addressing plastic pollution.

Keywords

Polystyrene beads, MNPs, live cell imaging, macrophages, transmission electron microscopy

Graphical Abstract

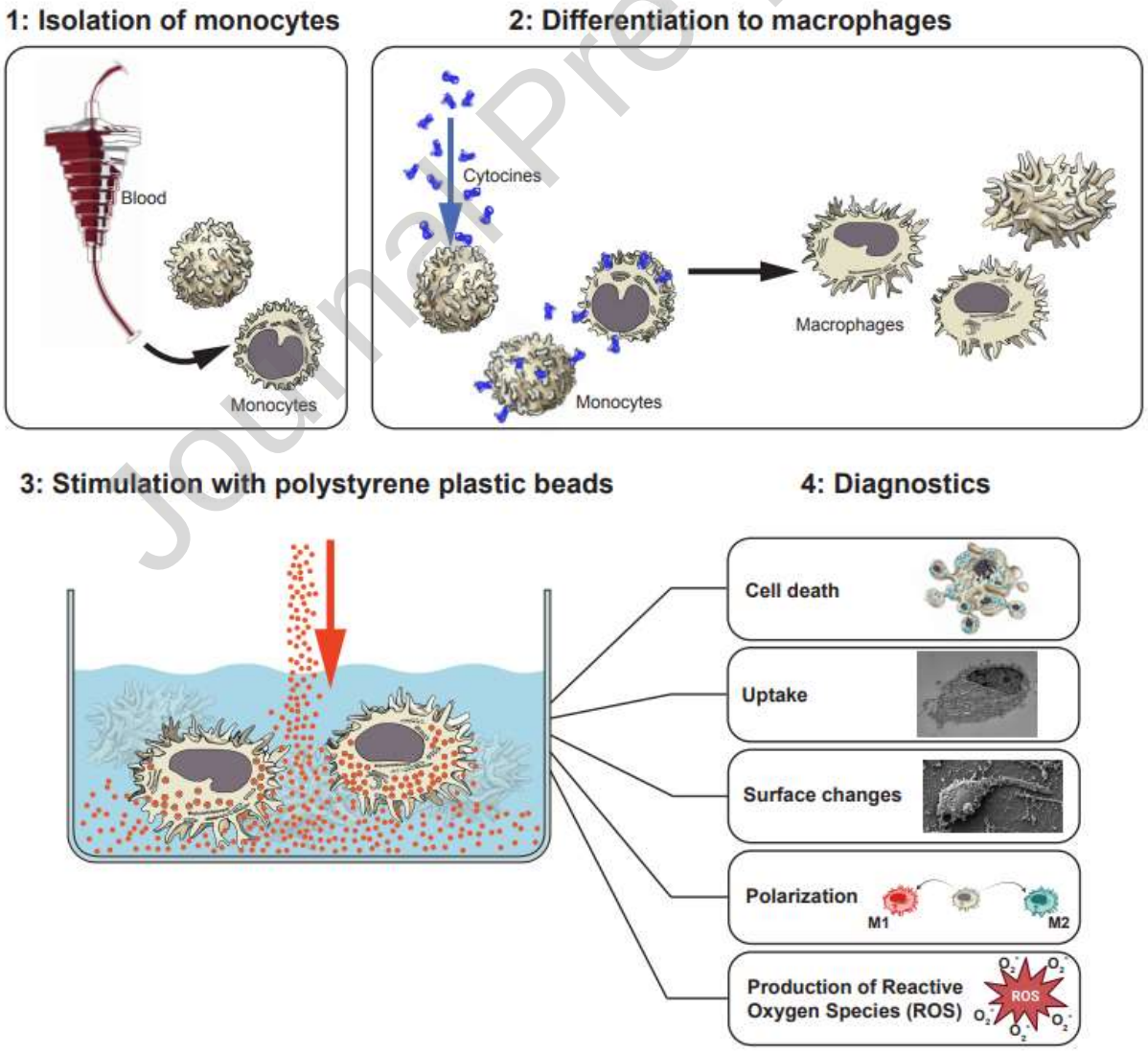

Introduction

The ubiquitous presence of micro- and nanoplastics (MNPs) in the environment has captured the interest of the scientific community, prompting an investigation into the potential impact of this pollution on human health. MNPs have been detected all over the world (1). They can be found in oceans (5), the atmosphere of large cities such as Shanghai (6) or of rural areas (7) and in agricultural soil (8). Studies working with animal models showed that exposure to microplastics (MPs) leads to accumulation of particles in different organs of mice (9) or reduces intestinal mucus (10). Further, for different human cell lines induction of apoptosis is reported (11). These observations elucidate that a possible harm to human health is mediated through exposure to MNPs, emphasizing the need of research in this field.

Plastic can even be found in human blood in an average concentration of 1.6 µg/mL (12). The type of plastic detected in human blood included styrene, a pyrolysis product of polystyrene (PS) or other polymerized styrene, which was found in 8 out of 22 samples (12). Therefore, we focused on PS in this study. PS is a thermoplastic, composed of styrene monomers. It is often used for food packaging and PS monomers can also migrate into food (13).

Concerning potential pathways how MNPs can possibly enter the human body and correspondingly also human blood, three mechanisms are usually discussed: via the gastrointestinal tract, through inhalation (14, 15) or transdermally (2). Potentially harmful substances have to pass the barriers of these organ systems, before entering the human body. Three layers compose the intestinal barrier, combining secretory products, gut microbiota, humoral components, an anatomic barrier built by the intestinal epithelium and immune cells, such as macrophages (16, 17). In the lung, the air-blood barrier is formed by endothelial cells and alveolar epithelial cells and alveolar macrophages are attached to the epithelial surface (18). Particles of a size smaller than 2.5 µm are able to reach the alveoli, however, the mucus layer on top of the epithelium, containing for example such small particles, is constantly transported towards the nasopharyngeal area and is swallowed afterwards. The skin's barrier is the result of a physical barrier formed by the epithelium, a humoral barrier mediated through antimicrobial peptides, a chemical barrier due to its' slight acid pH and an immunological barrier represented by different immune cells such as Langerhans cells, macrophages or mast cells (19). As this description shows, macrophages play an important role in all these barriers as one decisive component of innate immunity. They are part of the so-called professional phagocytes that are responsible for removal of microorganisms in the human body (20). Because of their key role in the different barriers of the human body, macrophages were chosen for further investigation. The importance of macrophages was also emphasized by Jeon et al. (21) stating that macrophages might be the decisive cell type for the influence of orally ingested MPs.

To study human macrophages, the THP-1 cell line derived from a patient with acute monocytic leukaemia is widely used. The cells of a cell line are immortalised and because they are cheap, easy to handle and constantly available, they are broadly used. Alternatively, human macrophages can be obtained from donors via isolating them from peripheral blood mononuclear cells (PBMCs). Since they are of natural origin, individual variations can occur, complicating analyses and interpretation (22). However, the malignant background of cell lines that divide without Hayflick limit narrows the conclusions, which can be drawn from their analyses, since they might differ in some properties from pristine cells (23). Therefore, studying *ex vivo* human macrophages can provide a more reliable insight into the possible consequences of MNPs on the human body. Thus, one focus of this study was to establish an *in vitro* model to study effects of MNPs on human macrophage behaviour obtained by differentiating monocytes isolated from PBMCs (dMPHs). Uptake of PS by murine macrophages and human macrophages derived from THP-1 cells was already observed (24–26) prompting the question whether pristine human macrophages take up PS as well. To visualize intracellular non-fluorescent PS micro- and nanobeads (MNBs) in differentiated THP-1 (dTHP-1) cells and dMPHs transmission electron microscopy (TEM) was used. In addition, scanning electron microscopy (SEM) and live cell imaging were performed for dMPHs.

Macrophages are not only responsible for removal of internal waste but are also effectors of cell-mediated immunity because of their ability to present antigens and to release pro- and anti-inflammatory cytokines (27, 28). Their contribution to different inflammatory diseases such as diabetes, cancer or atherosclerosis is subject of many studies (28). To examine whether a possible uptake of MNPs by human macrophages affects their immunological function, possible adverse effects of PS MNBs on human macrophages were investigated. These included the influence of PS MNBs on metabolic activity (dTHP-1), polarization of macrophages (dMPHs), cytotoxicity (dTHP-1, dMPHs) and generation of reactive oxygen species (ROS)(dMPHs).

Methods

The human monocytic cell line THP-1 was used to check if the applied TEM protocol works to visualize the uptake of non-fluorescent PS MNBs. Additionally, the influence on metabolic activity and cytotoxicity was measured. Since one of the main objectives of this study was to establish an *in vitro* model to study effects of MNPs on human macrophage behaviour, further experiments (TEM, SEM, live cell imaging, influence on polarization, production of ROS and cell viability) were performed using dMPHs extracted from Leukocyte Reduction System cones (LRSC) of healthy, anonymous donors having undergone a strict health check by the Transfusion Medicine and Hemostaseology Department of the Universitätsklinikum Erlangen, Germany. The permission to use these LRSCs was given by the ethics committee of the Friedrich-Alexander-Universität Erlangen-Nürnberg (ethical approval no. 48_19B), according to the rules of the Declaration of Helsinki in its current form.

Cell line THP-1

Cells of the human THP-1 cell line (ATCC, Manassas, USA) were differentiated into dTHP-1 following standard procedures (22). THP-1 cells were differentiated using phorbol 12-myristate 13-acetate (PMA, 25 ng/mL) in R10 medium (10 % FBS, 1 % Penicillin/Streptomycin in RPMI-1640 medium (Sigma-Aldrich, St. Louis, MO, USA)) over 72 hours in a density of 10000 cells per well in a 96-well plate.

Stimulation of dTHP-1 with polystyrene MNPs

dTHP-1 were exposed to PS MNBs (Polybead® microspheres, Polysciences, Warrington, USA) of different diameters and concentrations. Cells not exposed to PS MNBs served as controls. Higher concentrations than the currently physiological concentration of 1.6 µg/mL were included in the analyses to investigate concentration-dependent effects. TEM pictures were taken according to the steps outlined in section 2.6, metabolic activity and cytotoxicity (see 2.3) were measured after different timepoints. The chosen diameters, concentrations of PS MNBs and timepoints of each analysis are specified in Table 1.

Table 1: Overview of the conditions for each method used to examine dTHP-1

Experiment	Diameter (µm)	Concentration (µg/mL)	Timepoints (hours)
TEM	0.5, 1 and 3	37.5	24
		150	
		750	
		1500	
Metabolic activity	0.5, 1 and 3	37.5	24
		75	
		150	
		375	

		750	
		1500	
Cytotoxicity	0.5, 1 and 3	37.5	24, 48, 72
		75	
		150	
		375	
		750	
		1500	

.

Metabolic activity and cytotoxicity of stimulated dTHP-1

Metabolic activity of the stimulated dTHP-1 cells was assessed with the alamarBlue™ Assay (Invitrogen AG, Carlsbad, CA, USA). After 24 hours of exposure to PS MNBs, the medium was discarded, and cells were incubated under standard conditions with alamarBlue™ reagent (1:10 in differentiation medium) for 3 hours. Only medium with alamarBlue™ served as a blank. Absorbance was detected at 560 nm using the iMark Microplate Absorbance Reader (BioRad, Hercules, USA). Metabolic activity of controls was defined as 100 %. Cytotoxicity was measured using the CyQUANT LDH Cytotoxicity Assay (Invitrogen) and results were calculated (% cytotoxicity) according to the manufacturer's protocols. Negative results were omitted.

Monocyte isolation and differentiation of human macrophages

All steps were performed following the protocol of Wedekind et al. (29). PBMCs were separated from a LRSC using density gradient centrifugation. $CD14^+$ monocytes were isolated through magnetic activated cell sorting (MACS, Miltenyi Biotec, Bergisch Gladbach, Germany), according to the manufacturer's information. The naïve monocytes were seeded into 6-well plates at a concentration of $1.5 * 10^6$ cells per well. The differentiation into dMPHs was performed with macrophage-colony stimulating factor (M-CSF, 100 ng/ml, PeproTech, USA) in R10 medium. Cells were incubated under standard culture conditions for 6 days (37 °C, 5 % CO_2, Incubator MCO-230AICUV-PE, PHCBI, Tokyo, Japan). On day two and five, 500 µL R10 medium with M-CSF (100 ng/mL) were added. The detection of the surface proteins CD14, CD11b and CD68 by flow cytometry served as verification of macrophage purity (30).

Macrophage stimulation and pre-polarization

On day six, the supernatant was discarded, and the dMPHs were exposed to different substances (plastic stimulation or polarization in M1 or M2 macrophages) dissolved in 1 mL R10 medium. The stimulation with PS MNBs was carried out by using different diameters and concentrations of the same PS MNBs used to stimulate dTHP-1 (Polybead® microspheres, Polysciences, Warrington, USA). Unstimulated dMPHs were polarized to M1-dMPHs by adding Lipopolysaccharide (LPS, Sigma Aldrich) or to M2-dMPHs by adding IL-4 (Miltenyi Biotec). For the performed experiments, the observed substances, diameters of PS MNBs, concentrations and timepoints of analyses can be found in Table 2. dMPHs only exposed to R10 medium served as controls for all

experiments. Stimulated cells were incubated under standard culture conditions until the different analyses were carried out.

Table 2: Overview of the conditions for each method used to examine dMPHs

Experiment	Stimulant	Concentration (µg/mL)	Timepoint (hours)
TEM	PS beads Ø 0.5 µm	1.04	2, 24
		1.6	48
		10	24, 48
		37.5	2, 8, 24, 48
		75	2, 8, 24, 48
		375	2
		1500	2
	PS beads Ø 1 µm	37.5	2
		375	
		1500	
	PS beads Ø 3 µm	37.5	
		375	
		1500	
SEM	PS beads Ø 3 µm	10	24, 48
		37.5	
dMPH polarization, ROS (H_2DCFDA and Griess Assay)	PS beads Ø 0.5 µm	1.6	
		37.5	

Experiment	Stimulant	Concentration (µg/mL)	Timepoint (hours)
	IL-4	0.02	
	LPS	1	
Cell viability	PS beads Ø 0.5 µm	1.6	
		37.5	
live cell imaging	0.5 µm	1.6	individual durations
		37.5	

.

Transmission electron microscopy and scanning electron microscopy

To be able to visualize the non-fluorescent PS MNBs intracellularly, TEM was performed. Therefore, dTHP-1 and dMPHs were washed with PBS and fixed with Indium Tin Oxide (ITO) solution. Samples were dehydrated in an ascending ethanol series and embedded in Epon (Carl Roth, Karlsruhe, Germany). Ultrathin sections were stained using uranyl acetate and lead citrate and then ready for TEM analyses (JEM 1400 Plus; JEOL Germany GmbH, Freising, Germany). For SEM analyses of dMPHs surface the cells were initially seeded on cover slips. All other preparatory steps were equal to the preparation for TEM analyses. Protocols for TEM and SEM adhered to the guidelines outlined in the publication by Hampel et al. (31). dMPHs were examined with a scanning electron microscope (Jeol JSM-IT 300; JEOL, Tokyo, Japan).

Live cell imaging

dMPHs were seeded into µ-dishes at a concentration of $1.0*10^6$ or $0.5*10^6$ cells per dish and treated as mentioned in 2.4. On day six, the remaining medium was removed, PS nanobeads (NBs, 0.5 µm) were added, and the imaging was started using the Nanolive 3D CX-F microscope for live cell imaging (Nanolive SA, Tolochenaz, Switzerland). Exposure to PS NBs in a concentration of 1.6 µg/mL was monitored for about 24 h (n=3) and 37.5 µg/mL were filmed for 48 h (n=1). To edit the videos STEVE microscopy software was used. The non-fluorescent PS NBs were digitally stained based on visual perception. Videos were created out of pictures taken from one slice of the three-dimensional dMPHs (n=4) using ImageJ software.

Cell viability

After incubation with PS NBs (0.5 µm) for 24h and 48h and harvesting with Trypsin (GIBCO Life), cell viability was analysed by AnnexinV (AxV, GeneArt, Regensburg, Germany) and Propidium Iodide (PI, Sigma Aldrich) staining. Analyses were performed with the CytoFLEX S flow cytometer (Beckman Coulter, Brea, CA, USA) and Kaluza software. AxV^-, PI^- cells were defined as viable, AxV^+, PI^- as apoptotic, and AxV^+, PI^+ as necrotic cells (29). The gating strategy is displayed in Fig. 8**B**.

Polarization analyses by flow cytometry

Cells were harvested using a cell scraper and incubated with two different antibody panels, one fully stained panel and panel for background control. The background control panel included antibodies against CD11b (BV650, BioLegend, San Diego, CA, USA), CD68 (AF488, BioLegend), CD14 (PerCP-Cy5.5, BioLegend) and

a zombie NIR antibody (BioLegend). This served as a control to verify dMPH purity since they were differentiated from PBMCs. In addition, the fully stained panel contained antibodies against CD163 (PE-Dazzle, BioLegend), and CD206 (APC, BioLegend) for M1-polarization and HLA-DR (KO, Beckman Coulter) and CD80 (PE-Cy7, BioLegend) for M2-polarization. They were analysed using flow cytometry (CytoFLEX S, Beckman Coulter) and Kaluza Software. For Background correction, the median fluorescence intensity of the background control panel was subtracted from the fully stained panel. The gating strategy is displayed in Fig. 9**A**.

Reactive oxygen species production

Dichlorodihydrofluorescein-diacetat staining

After incubation with PS NBs (0.5 µm) for 24h and 48h, general ROS production was analysed with Dichlorodihydrofluorescein-diacetat staining (H_2DCFDA, 2 µmol/mL, Invitrogen, Carlsbad, USA). Cells not exposed to PS NBs served as controls and serum free medium (RPMI-1640, Sigma-Aldrich) without H_2DCFDA served as blanks. The staining was incubated for 90 minutes in the incubator. Cells were harvested using a cell scraper. Fluorescence of the cells dissolved in PBS with PI (1 µL/mL) was measured using flow cytometry (Beckman Coulter). For analyses Kaluza software was used (gating strategy is displayed in Fig. 10**A**) and background correction was carried out by subtracting the medium fluorescence intensity of blanks without H_2DCFDA from cells exposed to H_2DCFDA.

Production of Nitric oxide

The supernatant of the cell culture of dMPHs was centrifuged after 24 and 48 hours and stored at -20°C for further analyses. Production of nitric oxide was measured in a microplate assay using Griess reagent (Promega, Madison, USA), according to the manufacturer's instructions. Shortly, the culture supernatant was thawed, incubated for 10 minutes with Sulfanilamide Solution in the dark and then incubated for another 10 minutes with N-1-naphtylethylenediamine dihydrochloride (NED) in the dark. Standards were diluted in R10 medium. Absorbance was measured at 540 nm using a BioTek Epoch Microplate Spectrophotometer (Agilent, Santa Clara, USA).

Statistical analyses

Statistical analyses were performed with GraphPad Prism 8. For dTHP-1 experiments, tukey's multiple comparisons test was performed to compare all groups exposed to PS MNBs and controls (not exposed to any substance). For metabolic activity, activity of controls was defined 100 %. To assess the influence of MNBs size on cytotoxicity, results of different sizes of PS MNBs were compared and to assess the influence of duration, all time points were compared with each other. For experiments with dMPHs, a Kruskal–Wallis test was performed to compare all groups exposed to stimulants against the control not exposed to any substance with Dunn's correction for multiple testing. Significance is indicated as * $p<0.05$, ** $p < 0.01$, *** $p<0.001$, **** $p<0.0001$.

Results

Cellular uptake of Polystyrene MNBs by dTHP-1 influences metabolic activity and cytotoxicity

The studies of dTHP-1 showed uptake of PS MNBs of all sizes (0.5 µm, 1 µm, 3 µm, Fig. 1**A**) and thus determined our protocol for further analyses of PS-stimulated dMPHs from LRSC. Metabolic activity of the dTHP-1 cell line after exposure to PS MNBs of different sizes and concentrations was assessed with an alamarBlue™ Assay. This assay utilizes Resazurin, a cell-permeable and non-fluorescent substance, which is reduced to a fluorescent molecule upon entering living cells (32). Figure 1**B** shows the metabolic activity of dTHP-1 cells under the influence of PS MNBs compared to the controls' activity (100 %). PS microbeads (MBs, 1 µm, 3 µm) increased metabolic activity significantly unlike PS NBs (0.5 µm) when compared to controls. Higher concentrations of PS MBs were associated with a significant decrease in metabolic activity when compared to lower concentrations of the same size. P-values of all comparisons can be found in Table 3, Supplementary. Thus, metabolic activity increased in cells exposed to PS MBs (1µm, 3 µm) in intermediate concentrations.

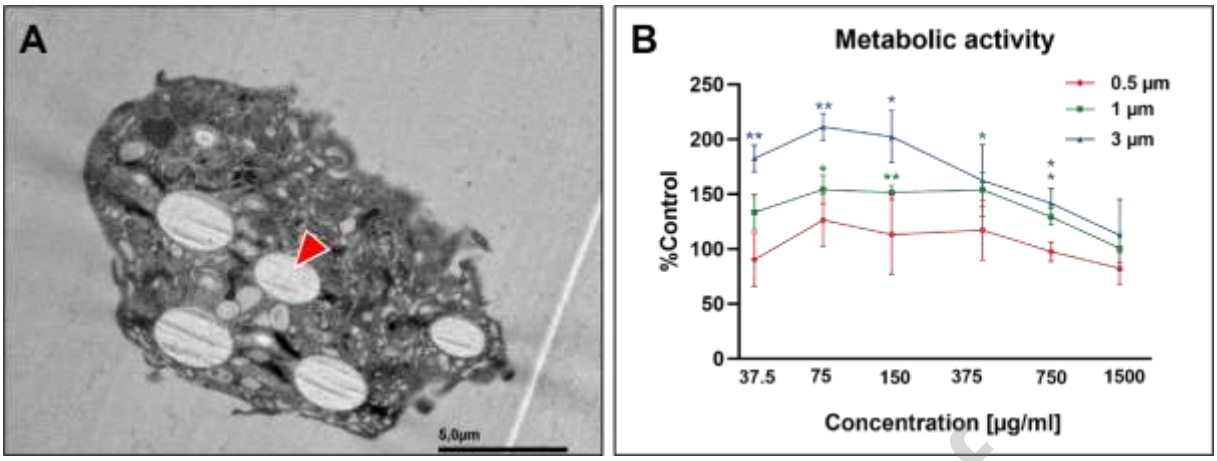

Figure 1: TEM picture and analyses of metabolic activity of dTHP-1 **A** TEM picture showing (five) intracellular PS MBs (3 µm) in a dTHP-1 cell after incubation with 37.5 µg/mL PS MBs for 24 hours. The arrowhead points at an intracellular PS MB. **B** Metabolic activity of dTHP-1 cells exposed to PS MNBs in ascending concentrations (shown on the x-axis) and diameters (0.5 µm, 1 µm and 3 µm) compared to the control's activity, which was set as 100 %. Significances shown here only refer to comparison with the controls. The metabolic activity was measured using an alamarBlue™ assay (Invitrogen). A significantly increased metabolic activity was observed for MBs (1 µm, 3 µm) and concentrations up to a concentration of 750 µg/mL. For NBs (0.5 µm) this increase was not observed. Higher concentrations of PS MBs are associated with a significant decrease in metabolic activity when compared to lower concentrations of the same size. P-values can be found in Table 3, Supplementary. n= 4, standard deviation shown. * $p<0.05$, ** $p < 0.01$

For the assessment of cytotoxicity, the release of Lactate Dehydrogenase (LDH) was examined. LDH is a cytosolic enzyme which is released into cell culture medium upon damage of the cell membrane (33). Based on LDH release, cytotoxicity of PS MNBs was calculated. PS NBs (0.5 µm) had significant impacts on cytotoxicity with ascending concentrations after all timepoints when concentrations were compared to the control (equals 0%) or to lower concentrations (n=3-4, Fig. 2, **A**). PS MBs (1 µm) also show this effect, however not as distinct as 0.5 µm NBs and rather after longer exposure periods (48 hours, 72 hours). PS MBs (3 µm) significantly increased cytotoxicity in higher concentrations when compared to the control especially after 48 hours. Analyses concerning the influence of size showed a significant decrease in cytotoxicity for PS MBs (1 µm, 3 µm) when compared to PS NBs (0.5 µm). 3 µm MBs revealed a significant decrease in cytotoxicity when compared to 1 µm MBs in some measurements (Fig. 2**B**). Comparison of the different timepoints showed a tendency towards a significantly higher cytotoxicity for longer exposure periods, especially when 48 hours were compared to 24 hours (Fig. 2**C**). An incubation for 72 hours only increased cytotoxicity significantly when compared to 48 hours of exposure in the highest concentration of 1500 µg/mL. P-values of all comparisons can be found in Tables 4-6, Supplementary.

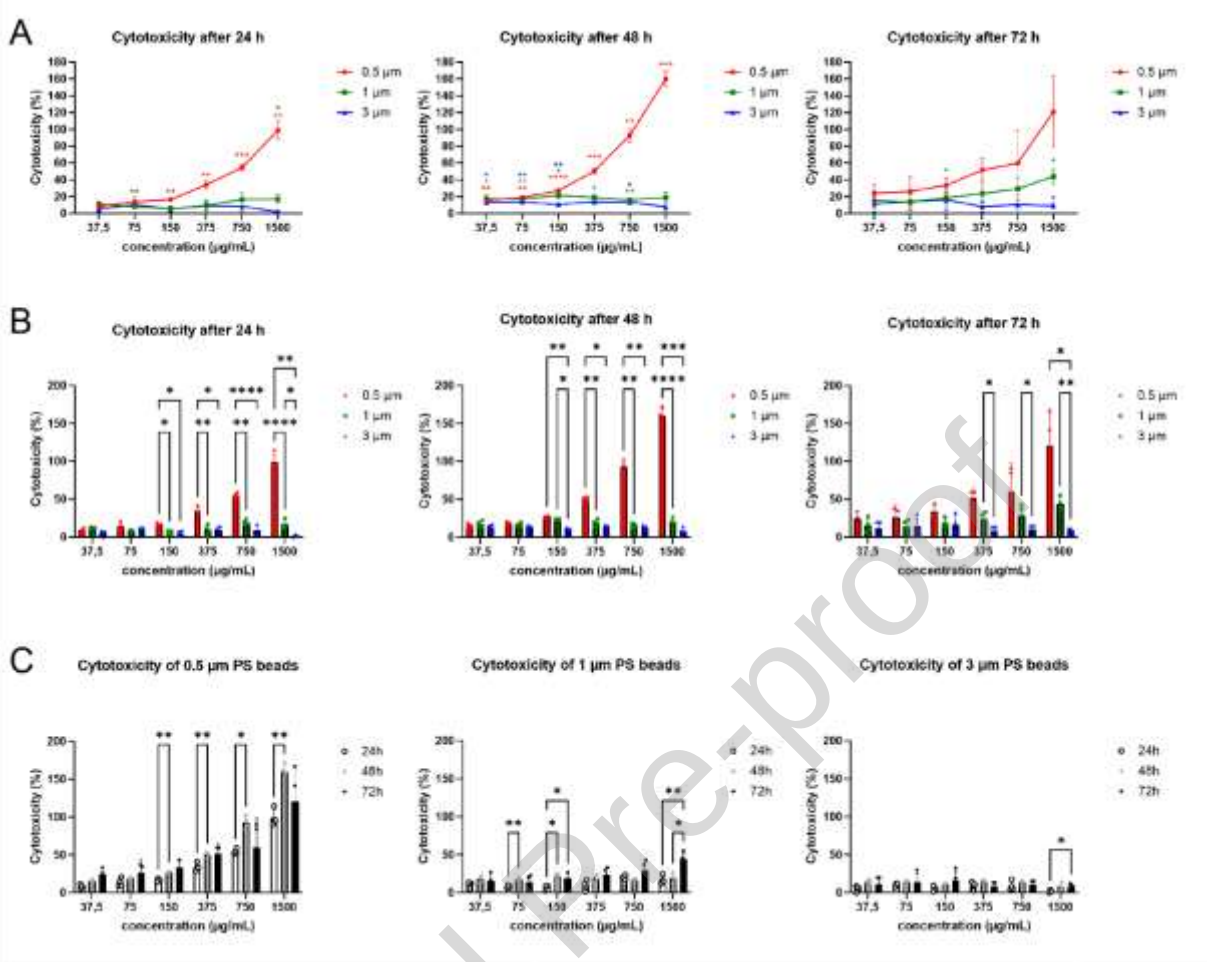

Figure 2: Cytotoxicity of PS MNBs on dTHP-1 **A Influence of different concentrations** Cytotoxicity of different concentrations (shown on the x-axis) and sizes (0.5 µm (red), 1 µm (green), 3 µm (blue)) after 24 hours, 48 hours and 72 hours on dTHP-1. Significances shown here only refer to comparisons with controls (equals 0 %). PS MNBs show an increasing cytotoxicity for increasing concentrations, especially PS NBs (0.5 µm). **B Influence of different sizes** Cytotoxicity of 0.5 µm, 1 µm and 3 µm PS MNBs in different concentrations (shown on the x-axis) after 24 hours, 48 hours and 72 hours on dTHP-1. PS MBs show a significant decrease in cytotoxicity when compared to PS NBs. **C Influence of different durations** Cytotoxicity after 24 hours, 48 hours and 72 hours of different sizes (0.5 µm, 1 µm, 3 µm) and concentrations (shown on the x-axis) of PS MNBs. An exposure for 48 hours shows significant increases in cytotoxicity when compared to 24 hours. The cytotoxicity was measured using a CyQUANT LDH Cytotoxicity Assay (Invitrogen). P-values can be found in Tables 4-6, Supplementary. n= 3-4, standard deviation shown. * $p<0.05$, ** $p < 0.01$, *** $p<0.001$, **** $p<0.0001$

Visualisation of Polystyrene uptake in dMPHs

On account of the results obtained from experiments using dTHP-1, the following experiments were performed using dMPHs. To demonstrate ingestion of non-fluorescent PS MNBs by dMPHs and their intracellular position after uptake, TEM, SEM, and live cell video microscopy were performed. TEM pictures were taken after 2, 8, 24 and 48 hours after PS MNB exposure to investigate time-dependency. In TEM, PS MNBs are visible as round to oval light grey structures. The appearance of blank space around the PS MNBs originates from cutting artefacts. Different sizes and concentrations were used to assess their influence on the uptake. Uptake of PS MNBs was observed under all conditions (Fig. 3, 4). Close-up TEM images were taken of PS MNBs to assess the intracellular localisation. No lipid-bilayer was detected surrounding the MNBs, which suggests that they are located in the cytosol.

Density of intracellular PS MNBs increased proportionally to their concentration. Live cell imaging showed the same effect and could moreover show the active engulfment of PS MNBs by the dMPHs. SEM confirmed the fully enclosed PS MBs by dMPHs. In TEM pictures, no major differences in the amount of intracellular PS

MNBs were observed after different timepoints. However, live monitoring showed that the longer the cells were exposed to PS NBs, the more could be detected intracellular. At higher concentrations, some PS MNBs were detected outside the cells (Fig. 3**F**), which was observed in the live cell imaging as well.

SEM was also used to assess sample density and visualize morphological changes of dMPHs. PS MBs with a diameter of 3 µm were chosen as a preliminary test had shown that 0.5 µm were below the detection rate of SEM. A high density of dMPHs was observed after 24 and 48 hours for the controls. Cell density was decreased after exposure to PS MNBs at both timepoints compared to the controls. The uptake of MBs was associated with morphological alterations of the cells, such as a shift towards a more circular shape. Changes in cell morphology were detected in the live cell imaging as well, with longer incubation the cells showed a more rounded shape. A complete circular shape of the cell was noted in SEM for the higher concentration of 37.5 µg/mL after 24 hours of exposure time.

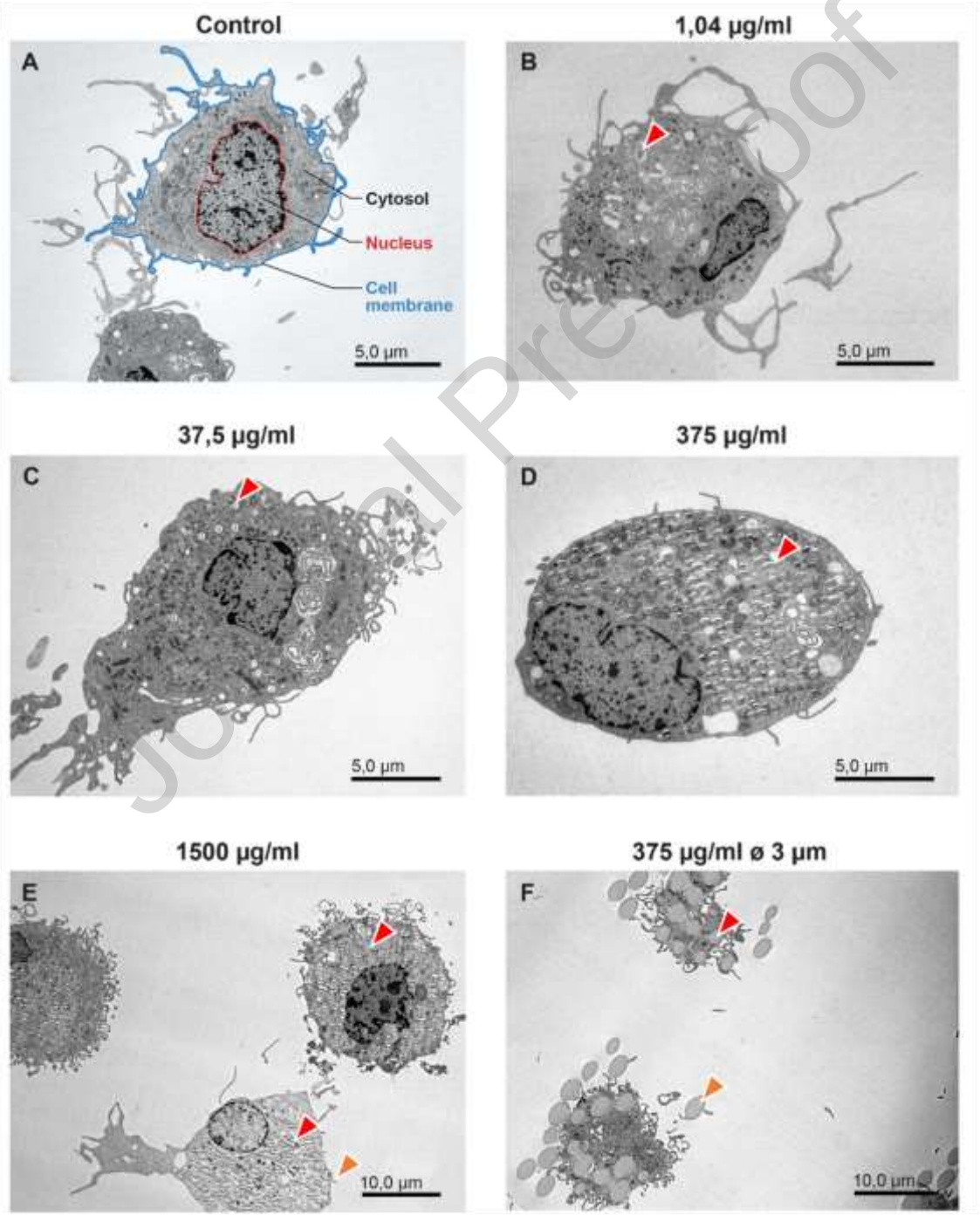

Figure 3: TEM pictures of dMPHs after 2 hours of stimulation with PS MNBs in different sizes and concentrations. PS MNBs are visible as round to oval light grey structures, red arrowheads point at intracellular PS MNBs, orange arrowheads at extracellular PS MNBs. **A** Unexposed dMPH serving as a control. Pictures **B-E** were taken from dMPHs exposed to PS NBs (0.5 µm). Concentrations of PS NBs ascend from B-E, resulting into a higher intracellular detection of NBs. Cells in picture **F** were exposed to PS MBs (3 µm). **E** and **F** both show extracellular PS MNBs.

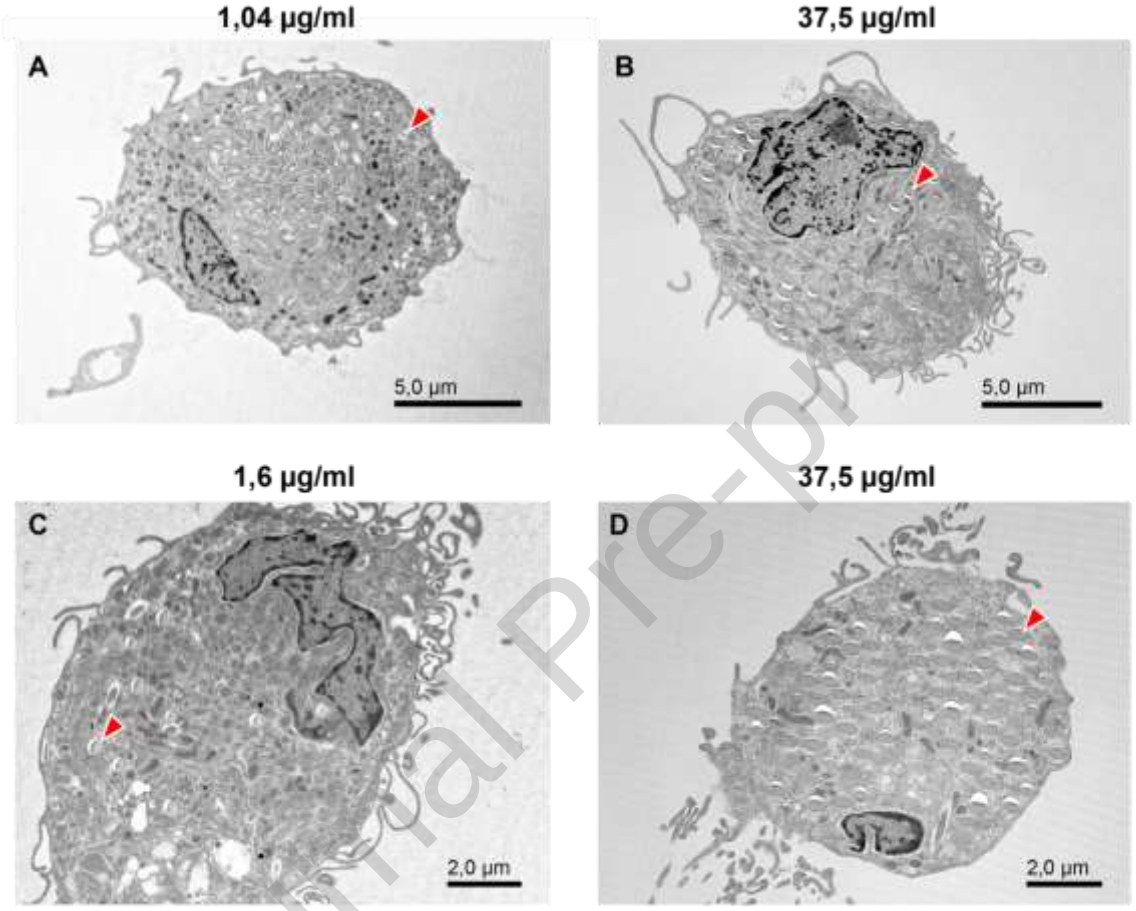

Figure 4: TEM pictures of dMPHs after 24 (**A** and **B**) and 48 hours (**C** and **D**) of stimulation with PS NBs (0.5 µm). PS NBs are visible as round to oval light grey structures, arrowheads point at intracellular PS NBs. **A** dMPH stimulated with PS NBs in a concentration of 1.04 µg/mL **C** dMPH stimulated with PS NBs in a concentration of 1.6 µg/mL. **B, D** dMPHs stimulated with PS NBs in a concentration of 37.5 µg/mL. For ascending concentrations of PS NBs, more intracellular PS NBs were observed.

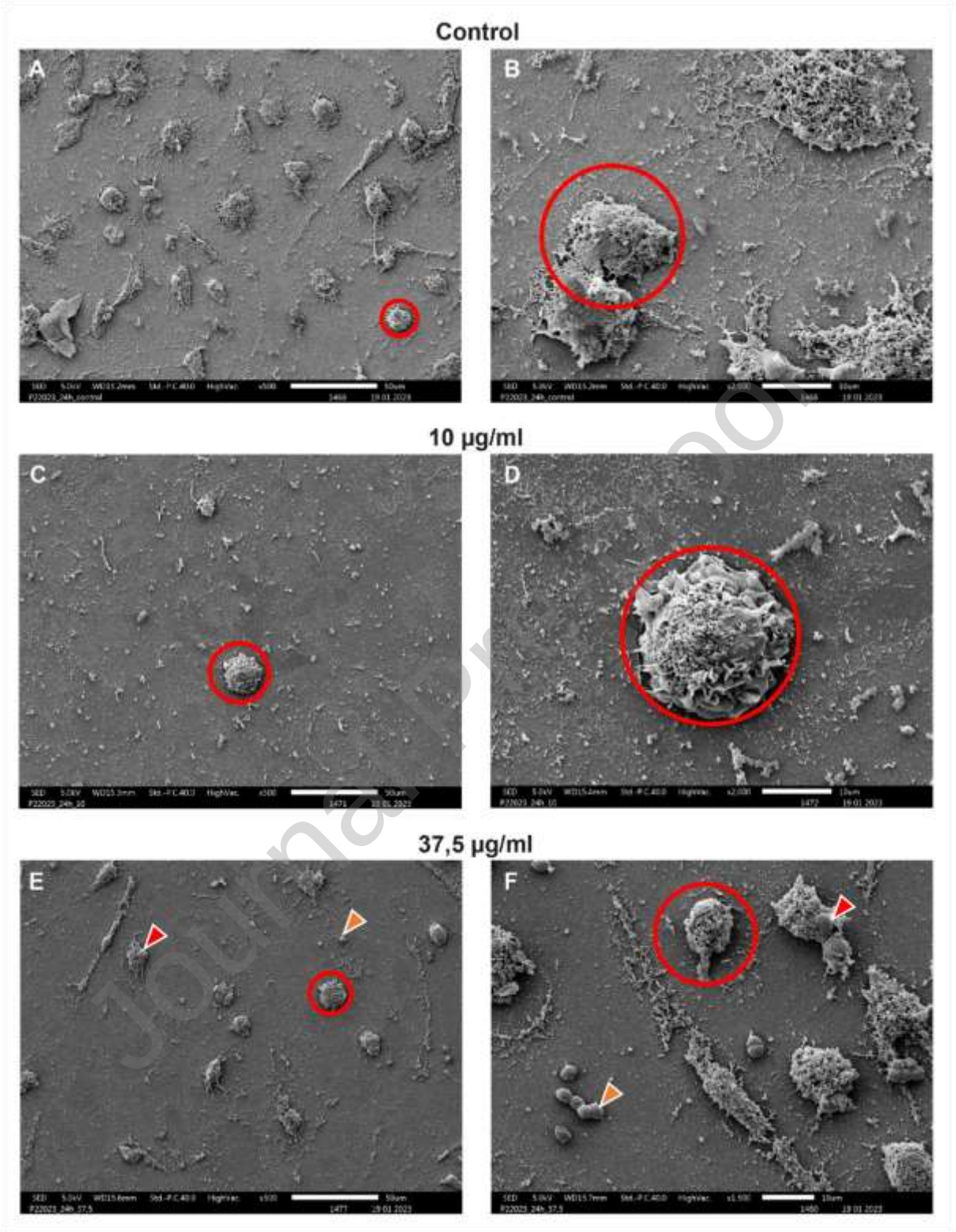

Figure 5: SEM pictures of dMPHs after 24 hours of exposure to PS MBs (3 µm). **A** and **B** were taken from controls, cells in **C** and **D** were exposed to 10 µg/mL PS MBs and cells in **E** and **F** were treated with 37.5 µg/mL PS MBs. dMPHs are exemplary encircled in red, red arrowheads point at intracellular PS MBs, orange arrowheads at extracellular PS MBs. PS MBs are visible as evenly round structures. In picture **E** and **F** the red arrowhead points at a macrophage enclosing a PS MB. Exposure to PS MBs causes decreased cell density and a circular shape of the dMPHs.

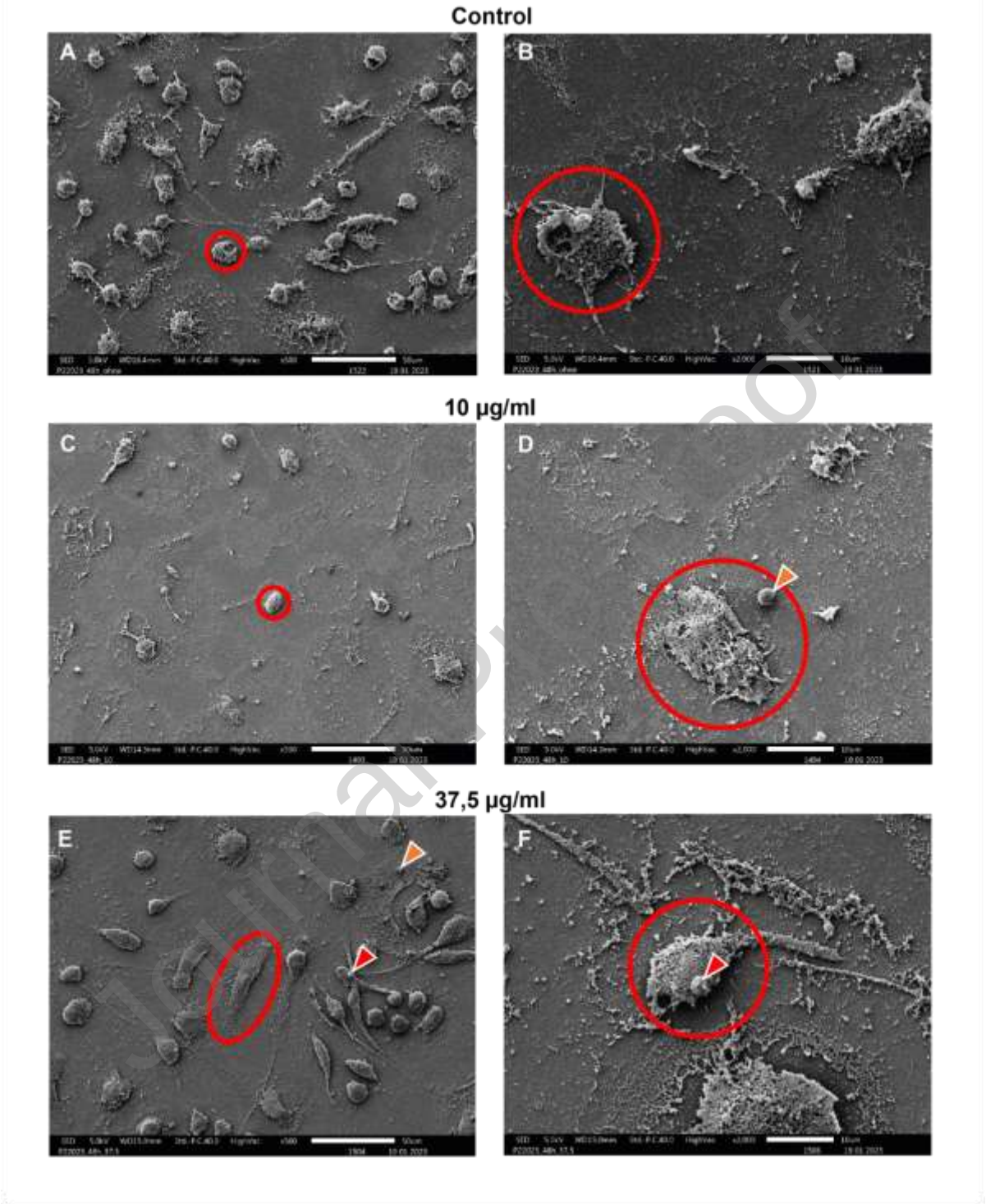

Figure 6: SEM pictures of dMPHs after 48 hours of exposure to PS MBs (3 µm). Control group is represented by image **A** and **B**. Cells treated with 10 µg/mL PS MBs are represented by image **C** and **D**. Images **E** and **F** illustrate the cellular morphology of cells treated with 37.5 µg/mL PS MBs. Exemplary dMPHs are encircled in red, red arrowheads point at intracellular PS MBs, orange arrowheads at extracellular PS MBs. PS MBs are visible as evenly round structures. In pictures **E** and **F** a macrophage enclosing a PS MB is shown.

PRINT VERSION

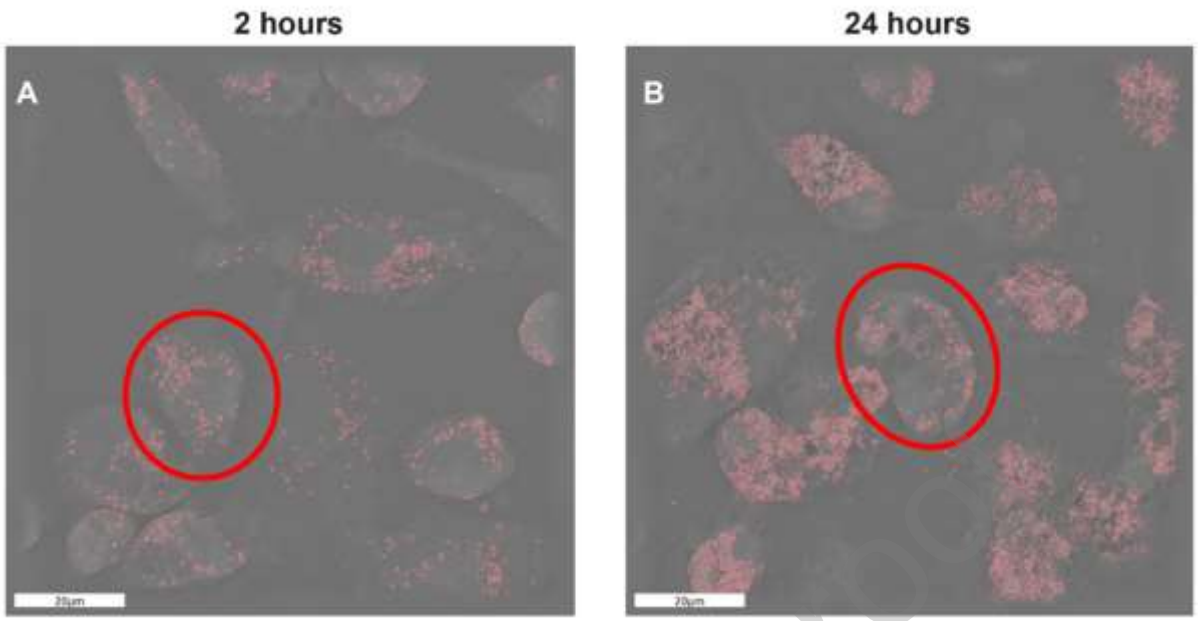

Figure 7: Pictures extracted from video material of dMPHs exposed to PS NBs (0.5 µm, pink) in a concentration of 37.5 µg/mL. The PS NBs were digitally stained based on visual perception. Duration of exposure: **A**: 2 hours, **B**: 24 hours. An increase of intracellular PS NBs can be observed for longer durations of exposure to PS NBs. Cells were observed for 48 hours in total.

ONLINE VERSION

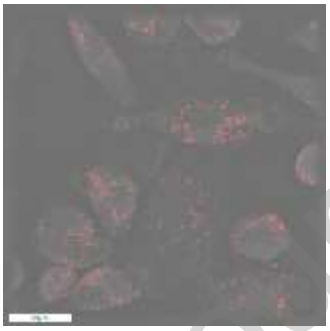

Video 1: dMPHs exposed to PS NBs (0.5 µm, pink) in a concentration of 37.5 µg/mL. PS NBs were digitally stained based on visual perception. Cells were observed for 48 hours in total. An increase of intracellular PS NBs can be observed for longer duration of exposure to PS NBs.

Exposure to Polystyrene NBs results into an increased number of necrotic cells

To distinguish between viable, apoptotic, and necrotic cells an AxV and PI staining was used. AxV binds to phosphatidylserine, which is exposed on the outer cell membrane of dead cells. The membrane of viable cells only contains phosphatidylserine on the inner part. To differentiate between apoptotic and necrotic cells, PI is used, as it can only diffuse through the membrane of necrotic cells (34). The results can be seen in Figure 8**C**. It shows the percentage of necrotic and apoptotic cells after 24 and 48 hours. After both timepoints, the majority of cells were viable. There was no significant influence of PS NBs on apoptosis. PS NBs at a concentration of 37.5 µg/mL caused a significantly higher number of necrotic dMPHs at both time points (n=4, p= 0.0285 for 24 hours, p=0.0121 for 48 hours, 0.5 µm).

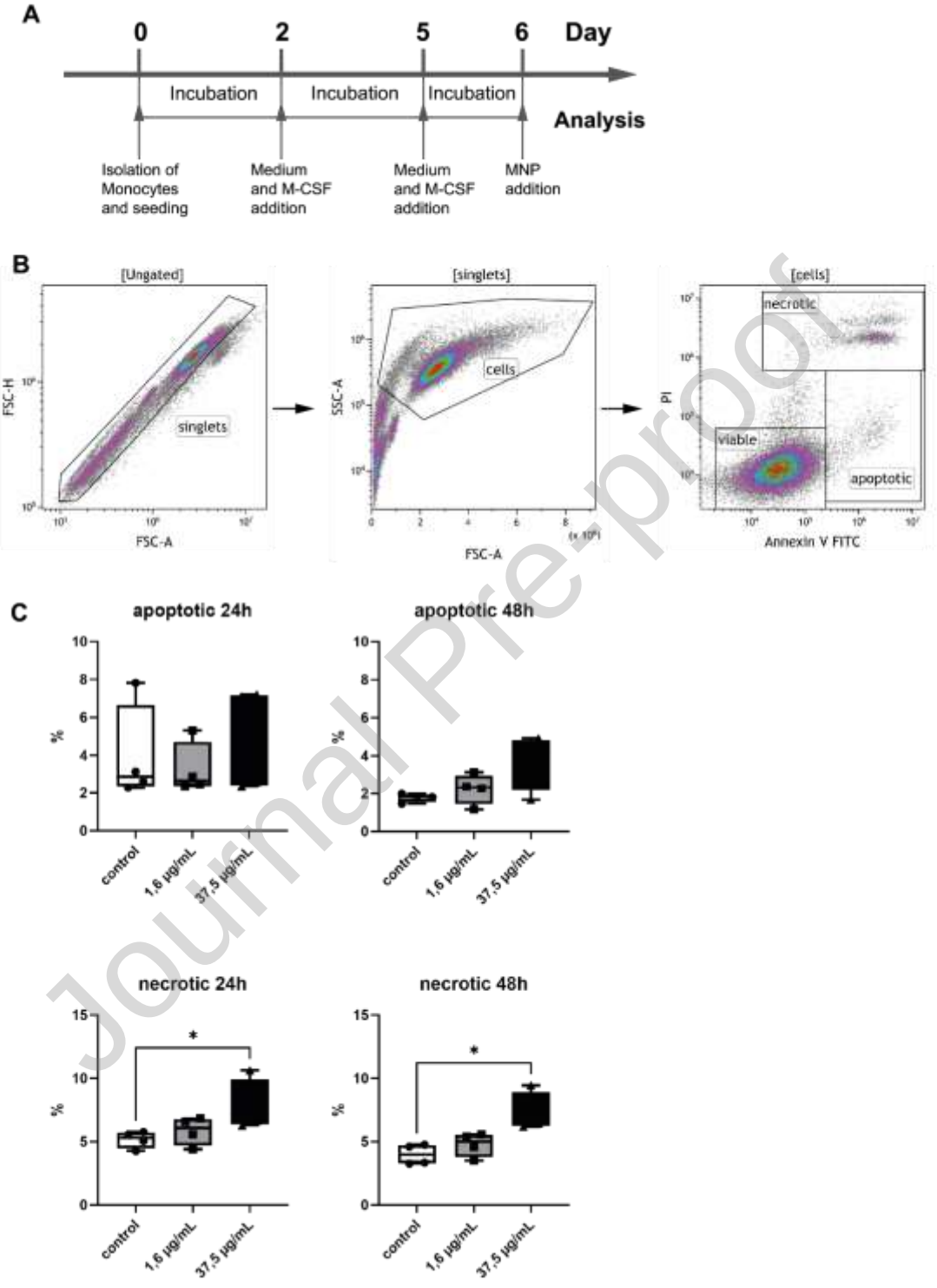

Figure 8: Analyses of cell viability of dMPHs after PS NB (0.5 µm) exposure **A** Timeline showing the essential steps for differentiation of macrophages isolated from a LRSC. **B** Cells were pre-gated on singlets (FSC-A/FSC-H), debris was excluded (FSC-A/SSC-A) and AxV^-, PI^- cells were defined as viable, AxV^+, PI^- as apoptotic, and AxV^+, PI^+ as necrotic cells. **C** Percentage of apoptotic and necrotic cells after 24 hours and 48 hours exposure

time to PS NBs (1.6 µg/mL and 37.5 µg/mL, 0.5 µm) or only R10 medium (control). Cell viability was assessed using AxV and PI staining. Numbers of necrotic cells are significantly increased after 24 and 48 hours of exposure time to PS NBs in a concentration of 37.5 µg/mL ($p= 0.0285$ for 24 hours, $p=0.0121$ for 48 hours). Kruskal-Wallis test and Dunn‘s multiple comparisons test; n=4, *$p< 0.05$.

Polystyrene NBs have no effect on macrophage polarization

To assess whether the dMPHs tend to develop into a rather pro-inflammatory (M1, also referred to as classical activation) or rather anti-inflammatory (M2, also called alternative activation) direction (35) after uptake of PS NBs, flow cytometric analysis of typical surface markers was performed. CD80 and HLA-DR are markers for M1 activation and CD163 and CD206 are markers for M2 activation (36). Only cells showing typical macrophage markers (see section 2.4) were included in the analyses. IL-4 polarizes macrophages to the anti-inflammatory subtype and LPS to the pro-inflammatory type (28) and were thus used as positive controls. Results are shown in Figure 9 (**B, C, E, F, H, I, K, L)**. CD80 was significantly increased by LPS after 24 hours (n=4, $p=0.0210$) and 48 hours (n=4, $p=0.0407$) and CD206 by IL-4 after 24 hours (n=4, $p=0.0356$). Expression of CD163 was significantly decreased by LPS after 48 hours (n=4, $p=0.0165$). The exposure to PS NBs in different concentrations showed no significant influence on marker expression. This shows that PS NBs have no impact on the polarization, although dMPHs are able to polarize.

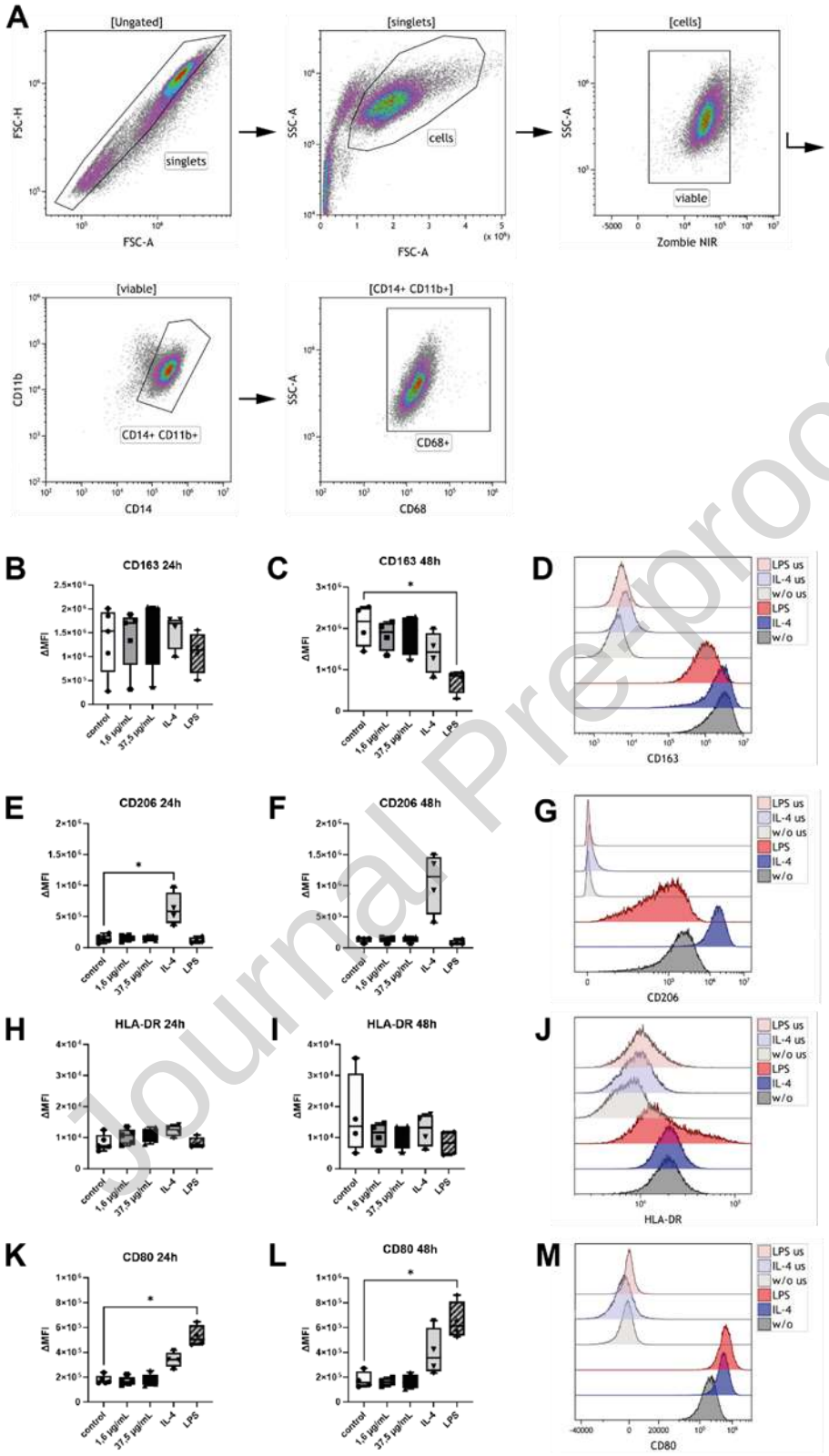

Figure 9: Analyses of dMPHs polarization after exposure to PS NBs (0.5 µm) **A** Cells were pre-gated on singlets (FSC-A/FSC-H) and viable cells based on morphological properties (FSC-A/SSC-A) and staining (Zombie NIR). Macrophages were identified by CD11b, CD14 and CD68 expression. **B,C,E,F,H,I,K,L** Background corrected (ΔMFI) median fluorescence intensity of CD163, CD206, CD80 and HLA-DR measured using flow

cytometry. **D,G,J,M** Representative data used for background correction for each marker. dMPHs were exposed to different concentrations of PS NBs (1.6 µg/mL and 37.5 µg/mL, 0.5 µm), IL-4 (20 ng/mL), LPS (1 µg/mL) or R10 medium (control) for 24 hours and 48 hours. A significant decrease of CD163 can be seen after 48 hours exposure to LPS ($p= 0.0165$). CD206 is significantly increased by IL-4 after 24 hours ($p= 0.0356$). Expression of CD80 is significantly increased after 24 hours and 48 hours of exposure to LPS ($p= 0.0210$ for 24 hours, $p= 0.0407$ for 48 hours). Exposure to PS NBs showed no significant influence on the expression of surface markers. Kruskal-Wallis test and Dunn's multiple comparisons test; n= 5 for cells exposed to PS NBs for 24 hours, n= 4 for cells exposed to PS NBs for 48 hours, IL-4 or LPS; *$p< 0.05$.

Nitrite, but not general reactive oxygen species, is increased by PS NBs in dMPHs

ROS production was analysed by H_2DCFDA staining and measuring the fluorescence with flow cytometry. H_2DCFDA diffuses into the cells, is modified by the cellular esterase and intracellular ROS can oxidize the resulting molecule (37), resulting in a fluorescent molecule. The results can be seen in Figure 10**B,C**, showing the median fluorescence intensity in dependence of the exposed substance. No significant influence on general ROS production after exposure to PS NBs, IL-4 or LPS was detected. A clear trend of an increased ROS production after exposure to LPS which served as a positive control, especially after 48 hours, is recognizable.

As H_2DCFDA staining measures several ROS (38), nitric oxide (NO) production as a specific type of reactive nitrogen species (RNS) produced by macrophages (39) was analysed in addition using the Griess reaction. This method indirectly quantifies NO production by measuring Nitrite and is a standard assay to assess NO production (40). A significant increase was observed for 37.5 µg/mL PS NBs after 24 hours (0.5 µm, $p=0.0486$, Fig 10**E**). All other stimulants showed no significant impact on NO production, although an increase is visible for the same condition after 48 hours as well (Fig. 10**F**).

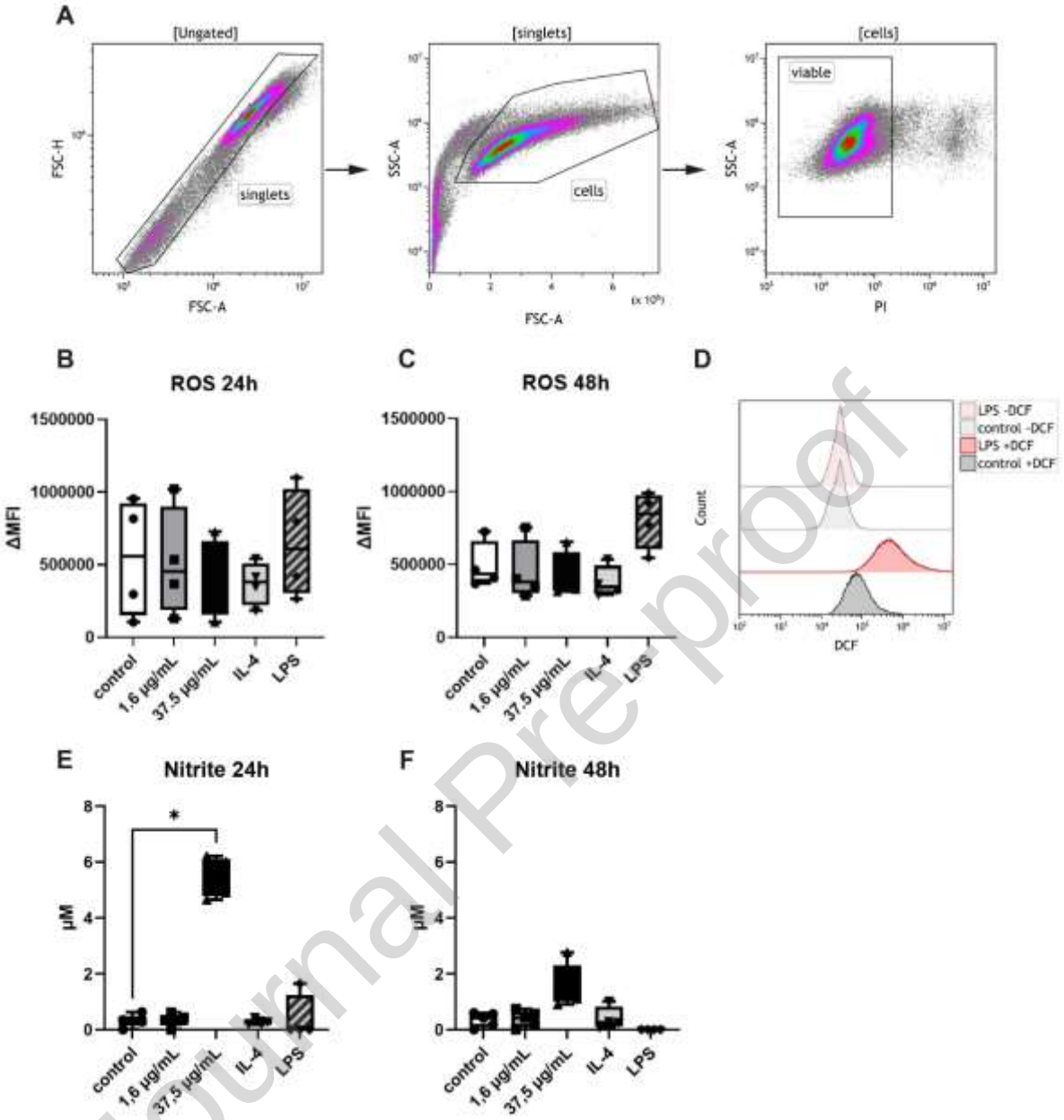

Figure 10: **A** Cells were pre-gated on singlets (FSC-A/FSC-H), debris was excluded (FSC-A/SSC-A) and viability of cells was assessed with a PI staining. **B-C** Background corrected mean fluorescence signals (y-axis) from H_2DCFDA staining, indicating the intracellular generation of ROS, for the different stimulation substances (x-axis) are shown. MPHs were exposed to PS NBs (0.5 µm, 1.6 µg/mL and 37.5 µg/mL), IL-4 (20 ng/mL), LPS (1 µg/mL) or R10 medium (control) for 24 and 48 hours. No significant influence on general ROS production was observed for any substance. Kruskal-Wallis test and Dunn‘s multiple comparisons test; n=4, *p< 0.05. **D** Representative data used for background correction. **E, F** Concentration of Nitrite (in µM) for the different stimulation substances are shown. MPHs were exposed to PS NBs (0.5 µm, 1.6 µg/mL and 37.5 µg/mL), IL-4 (20 ng/mL), LPS (1 µg/mL) or R10 medium (control) for 24 and 48 hours. A significant increase in Nitrite production was observed for 37.5 µg/mL (p=0.0486, 24 h). Kruskal-Wallis test and Dunn‘s multiple comparisons test; n=5 for controls and cells exposed to PS NBs, n=4 for IL-4 and LPS exposure, *p< 0.05.

Discussion

The physiological concentration of 1.6 µg plastic particles per mL blood found by Leslie et al. (12) was of major interest in this project to outline the potential consequences for the human body. Previous studies have shown that murine macrophages and THP-1 cells internalize PS MNPs (24–26, 41, 42). However, most studies

investigating the cellular internalization of MNPs used fluorescently labelled particles that do not resemble MNPs occurring in nature (43). Fluorescent labels may leach out from the particles leading to a false positive result or may even be toxic triggering adverse effects not originating from the particles per se (44, 45). Therefore, one goal of this study was the visualization of non-fluorescent PS MNBs in human macrophages by using TEM for the visualization of intracellular MNP. The results from this study using well-defined PS MNBs help understand the basic mechanisms and will enable to transfer the experimental approaches to other more environmentally relevant particle types used in future studies. Using TEM, no difference concerning the uptake between different sizes of PS MNBs or different timepoints was observed. A rapid uptake of PS NPs, which only moderately increased after 2 hours of incubation, was already observed before in dTHP-1 cells (46). Most PS MNBs have already been taken up within this period. To investigate time-dependency, live cell imaging was performed, and it showed that an increase of intracellular PS NBs correlates with a longer exposure period. With increasing concentrations of PS MNBs, an increasing amount of intracellular beads was observed, indicating that PS MNBs were taken up by dTHP-1 and dMPHs in a concentration-dependent manner, regardless of their size. Extracellular PS MNBs were observed for high concentrations such as 375 µg/mL after 2 hours of exposure time in TEM. This could indicate a saturation or time was not sufficient for a complete ingestion. For longer exposure times, only lower concentrations were investigated. PS NBs observed outside the cells in live cell imaging support the idea of a possible saturation. Although this observation could also be caused by cell death leading to the release of PS NBs or even an active process, the active release of PS NBs was not observed in live cell imaging; hence, a saturation of the cells is considered most reasonable. Assessment is aggravated because both methods reflect only one level of a three-dimensional system. Therefore, extracellular PS MNBs could also be located at a different level. This is also the most likely explanation why no extracellular PS NBs are visible at the beginning of live cell imaging. Thus, determination of an endpoint of uptake is not achievable and should be subject to future studies. Another interesting follow-up question is whether the uptake up to a saturation of PS MNBs impacts the ability of dMPHs to take up other particles or bacteria.

However, not only the size of the particles, concentration and time-dependent effects may determine their interactions and uptake by cells but also their physicochemical surface properties, like their zeta potential or surface coatings like a protein or eco-corona. Wieland et al. (47) recently showed that the zeta potential of the particles can be one of the driving factors of whether a particle interacts with a cell. They showed that the number of particles interacting with and their subsequent internalisation by cells increases with an increasing zeta potential. Furthermore, once the particles were coated with an eco-corona, their zeta potential became more negative which led to a higher likeliness to interact with cells and becoming internalized (43, 47). The particle-cell interaction and its internalization by cells is a pre-requisite for testing cytotoxicity and therefore the differences in particle-cell interactions due to the different particles' properties may consequently lead to differences in their cytotoxic potential. For instance, dTHP-1 cells treated with differently surface functionalized 50 nm PS NPs showed that aminated NPs were more cytotoxic and genotoxic than carboxylated or unmodified NPs (46). Furthermore, high concentrations of MP with a higher negative zeta potential can influence cell proliferation and induce higher cytotoxicity in murine macrophages compared to more neutral particles (48). This shows that using pristine PS MNBs underestimates the risks associated with MNPs, since the uptake and therefore also the effects of PS MNBs are influenced by environmental conditions. Therefore, using the PBMCs cell model established in this study will be highly relevant to be used in future studies including more complex MNP of different sizes, shapes, environmentally coatings and surface functionalisation.

Concerning the intracellular localisation of PS MNPs, it was found that in murine macrophages and dTHP-1 PS MNP was localized in the cytosol (26, 46). NPs and NBs were also found in the endoplasmic reticulum (26, 49). PS NBs were detected in endosomes of murine macrophages (49). In the present study, PS MNBs were also visualized in the cytosol by TEM but could not be detected in the endoplasmic reticulum or in endosomes. To further investigate this, staining of the different organelles, as implemented by Jasinski et al. (49), could be an option. The circular morphological changes observed in SEM and video microscopy suggest that the cells are undergoing a degree of stress or damage in response to the exposure. It is also possible that the cells were attempting to contain or isolate PS MNBs to minimize further harm to themselves or nearby cells. Another possibility is that the uptake of PS MNBs by the macrophages contributes to the observed changes in morphology and density, as cells engulf and internalize particles or other cells. However, especially the effects observed in the live cell imaging could also speak for an increased cell death due to PS NBs. Cellular toxicity of PS MNBs, resulting in cell death, may also explain the decrease in cell density (not quantified) observed in SEM after treatment with PS MBs.

In regard to a possible toxicity of intracellular PS MNPs, a reduction in viability of dTHP-1 cells is known for unmodified PS, amino-modified PS (50 nm, 52 nm) (46, 50) and carboxyl-modified PS (20 nm, 500 nm, 1000 nm) (51). Interestingly, no cytotoxic effects were observed for unmodified PS NBs (50 nm) (50) and NPs (50 nm, 200 nm, 500 nm) (26) or carboxyl-modified PS NPs (48 nm) (46) on dTHP-1 cells by other groups. Wolff et al. (52) observed a tendential decrease in cell viability of macrophages derived from human PBMCs upon exposure of PS MNBs. The analysis of cytotoxicity of PS MNBs for dTHP-1 reveals an increasing cell death for ascending concentrations of PS MNBs, indicating a concentration-dependent cytotoxicity. This association is particularly notable for PS NBs (0.5 µm). The observation that PS MBs of 3 µm did not increase cytotoxicity in higher concentrations after 24 hours can be explained by the observed smaller toxic effects of PS MBs (3 µm, 1 µm). The results show a size-dependency of PS MNBs' cytotoxicity, as a smaller size (0.5 µm) shows a higher impact on cytotoxicity. Within the beads classified as MBs, a larger size (3 µm) showed an even smaller cytotoxic effect when compared to 1 µm MBs. However, since larger particles in the same concentration as smaller particles contain a minor absolute number of particles, this decrease in cytotoxicity could also be explained by the total amount of PS MBs. Furthermore, a time-dependency was observed for dTHP-1, as after longer exposure times (48 hours, 72 hours) an increasing cytotoxicity was observed when compared to 24 hours exposure. Comparison of the two later timepoints showed no clear difference. Thus, these results indicate that PS MNBs have developed their cytotoxic effect after 48 hours of exposure. As primary cells allow a deeper insight in cell viability regarding the differentiation between apoptotic and necrotic cells than cell lines (23), analyses of dMPHs revealed a significant increase in necrotic cells for a higher concentration (37.5 µg/mL) of PS NBs (0.5 µm), supporting the idea of a concentration-dependency. Other studies confirmed these findings by reporting an induction of apoptosis and necrosis (53, 54) for non-human cells. Overall, a decrease in cell viability of macrophages was shown in this study for dTHP-1 and dMPHs, whereby investigations of dMPHs, in contrast to investigations of dTHP-1, provide more information about apoptosis and necrosis.

An explanation for differing results on cytotoxicity of PS MNPs from different suppliers is that general conclusions on the same size and type of plastic can only be drawn when physicochemical properties are taken into consideration (47, 48). Busch et al. (50) used PS NBs (50 nm) to investigate toxicity on dTHP-1 from the same supplier as the PS NBs used in this study (0.5 µm). A possible explanation for the contradictory results here could be the difference in size. The important role size of PS MNBs plays in the induction of cell death was shown in the cytotoxicity analyses in this work. A potentially higher effect of PS NPs is confirmed by other studies (3, 55). Another result from our study supports this hypothesis: dTHP-1 exposed to PS MBs (1 µm, 3 µm) had a higher metabolic activity, resembling a well-functioning cell. Increasing concentrations of larger PS MNBs did not show this increase of metabolic activity compatible with the observation of concentration-dependent effects. Similar observations were made for murine macrophages using the same 3 µm PS MBs (48). This can possibly be explained by the cells focusing their metabolism on uptake of PS MNBs. To evaluate the impact of different sizes, further functional tests with this novel *in vitro* model considering physicochemical properties and the coating with an eco-corona are necessary.

A common mechanism held responsible for the impact of MNPs on cells is the generation of ROS (56). This process is usually used by macrophages as a defence mechanism against bacteria and parasites (57), but an increase also correlates with oxidative stress and cellular damage such as oxidation of proteins (58, 59) and DNA (56). Therefore, the influence of PS NBs on production of ROS was of major interest to assess possible consequences on the human body. For MNPs, an increase in ROS production has been shown for different cell lines such as dTHP-1 cells, Raji-B cells and TK6 cells (21, 26) under exposure to different plastic particles, including PS. On the other hand, a reduction in ROS production was reported for carboxy-modified PS stimulated RAW264.7 mouse MPHs (42) and no increase in ROS production by THP-1 cells stimulated with PS NPs is reported by other groups (60). The results of our study do not show an increase in general ROS production after exposure to PS NBs, which matches the results of Lunov et al. (61) who used primary human macrophages stimulated with LPS before PS exposure and measured mitochondrial ROS. An explanation for the differing results can be the usage of different cell types or differences in particle size and/or particle characteristics, as size-dependent effects and an influence of the direct particle environments have been reported to influence ROS production (56).

Simultaneously, the results of this study show an increase in NO production in response to stimulation with PS NBs in a higher concentration. A significant impact was observed after 24 hours for 37.5 µg/mL and an increase of NO for this condition is still observable after 48 hours, showing that levels of NO are concentration-dependent and decrease after a longer exposure period to PS NBs. Prietl et al. (51) observed an increase in NO production

for mouse macrophages stimulated with Carboxyl PS and Wang et al. (3) observed a concentration dependent increase of NO for RAW264.7 macrophages stimulated with PS MNPs. The results of this study support the current state of knowledge on NO production induced by PS NBs using dMPHs for the first time. NO is a soluble gas with multiple functions in humans: NO has a vasodilatory effect and is produced by vascular endothelial cells; it is a neuronal messenger in the brain (62) and increased levels of NO are associated with diseases such as rheumatoid arthritis (63), systemic lupus erythematosus (64), and multiple sclerosis (65). In macrophages, NO interacts with various intracellular processes, for example it inhibits complex IV of the electron transport chain in mitochondria (66). By this, it influences the mitochondrial membrane potential and can have antiapoptotic effects which was found by Beltrán et al. (67). However, Beltrán et al. discuss that this effect might be influenced by duration of exposure to NO and that a longer inhibition of complex IV results in oxidative stress.

The differing results of this study concerning general ROS and NO production emphasize the necessity to distinguish between different kinds of ROS. If only general ROS production had been investigated, the effects of PS MNBs would have been underestimated. At the same time, assessing the consequences of an increased NO production again emphasized the complexity and diversity of interactions in the human body. Therefore, it might be too generalizing to only examine general ROS species and future studies should distinguish more clearly which exact type of ROS is influenced by MNPs.

As mentioned before, macrophages can be divided into two subtypes. Pro-inflammatory M1 macrophages are associated with a high production of IL-12 and IL-23 (68), whose release contributes for example to the emergence of intestinal bowel disease (69). At the same time, M1 macrophages are associated with anti-tumour effects (68, 70) and M2 macrophages have been related with tumour growth (68). These examples show how the microenvironment influenced by macrophages can have severe impacts on health, proving the importance to consider this aspect when investigating consequences of PS MNBs uptake by macrophages. In this study, M-CSF was used to differentiate macrophages, which induces a non-activated M0 state (52). To distinguish between the two subtypes of macrophages, identification of key surface markers is a well-established method. The changes of marker expression under the influence of IL-4 and LPS indicate that LPS polarizes dMPHs towards the M1 subtype and IL-4 stimulates them into the M2 direction (71). This proves that the method applied in this research detects polarization of dMPHs. The influence of unmodified PS NBs (0.5 µm) on the expression of surface markers in human dMPHs was explored. Collin-Faure et al. (24) and Merkley et al. (25) found changes in the expression of surface markers for mouse macrophages exposed to PS MNPs. This is different from the findings by Fuchs et al. (72), who isolated macrophages from human blood and pre-differentiated them into M1- and M2- macrophages before stimulation with carboxyl- and amino-functionalized PS NPs. The results showed no influence on the expression of M1 surface markers and reduced expression of CD163 and CD200R (both typical M2 markers (73, 74)) in M2 macrophages (72). Wolff et al. (52) recently showed a downregulation of M1 markers after stimulation with amino-modified and unmodified PS MNBs. The present study did not detect any change of surface marker expression under the influence of PS NBs. The outcomes of the studies with human macrophages differ strongly. One possible explanation for this might be donor variability. Another important aspect is, that *in vivo* nanoparticles are surrounded by protein coronas and the properties of the proteins also influence macrophages polarization (75). This effect could be even enhanced for environmentally relevant MNPs coated with an eco-corona. In conclusion, all these findings underline the importance of further research using dMPHs and considering protein- and eco-coronas as well as plastic characteristics for macrophage polarization.

Conclusion

This study validates the isolation of macrophages from PBMC's as a suitable method to investigate the influence of MNPs on human macrophages. Intracellular uptake of non-fluorescent PS MNBs was visualised with TEM and live cell imaging for the first time. The consequences of this uptake on dTHP-1 are a size- and concentration-dependent influence on metabolic activity and additionally a time-dependent effect on cell death. No effect on dMPHs polarization was observed for PS NBs, however dMPHs show a significantly increased necrosis after exposure to a higher concentration of PS NBs than the currently physiological concentration in our blood. The alterations of human macrophages observed in this study, especially for higher concentrations of PS MNBs, indicate that PS MNPs may interact with the finely tuned human immune system. This observation emphasizes the need to minimize the MNP concentration organisms are exposed to. The results of this study show that both, dTHP-1 and dMPHs, take up PS MNBs in a concentration-dependant manner which leads to

cytotoxic effects. In conclusion, the usage of dTHP-1 to study the effects of MNPs on human macrophages is suitable for orienting experiments. However, such observations should be confirmed by using dMPHs as they represent more physiological cells and allow more reliable conclusions concerning the effects on humans. The methods described in this study provide a basis for necessary future analyses to further investigate these influences and show that this is a sufficient macrophage *in vitro* model. With this model, the impact on human macrophages of more types of MNPs with different shapes and particle coronas that better reflect plastic taken up by humans can be studied. Knowing macrophages behaviour towards MNPs helps assessing the risk of MNPs for human health and take preventive action.

CRediT authorship contribution statement

M.Y.A.: Conceptualization, Investigation, Formal analysis, Writing - Original Draft, Writing - Review & Editing, Visualization, Validation. **I.I.:** Investigation, Formal analysis, Writing - Review & Editing. **M.R.:** Conceptualization, Methodology, Formal analysis, Writing - Review & Editing, Visualization, Validation, Supervision. **L.D.:** Conceptualization, Formal analysis, Methodology, Writing – Review & Editing, Visualization, Validation, Supervision. **C.M.:** Methodology, Resources, Writing – Review & Editing. **T.T.:** Methodology, Resources, Writing – Review & Editing. **C.A.:** Resources, Writing – Review & Editing. **F.P.:** Formal analysis, Writing – Review & Editing. **A.F.R.M.R.:** Writing – Review & Editing, Funding acquisition. **C.L.:** Writing – Review & Editing, Funding acquisition. **U.G.:** Conceptualization, Resources, Writing – Review & Editing, Supervision. **K.J.:** Conceptualization, Methodology, Formal analysis, Writing – Original Draft, Visualization, Supervision, Project administration. **F.P.:** Conceptualization, Resources, Writing - Review & Editing, Supervision, Funding acquisition, Project administration

Competing interests

The authors declare no competing interests regarding the publication of this article.

Funding

This work received funding from the European Union's Horizon 2020 Research and Innovation programme [grant number 965367 (PlasticsFatE)}. L.D. is funded by the Bundesministerium für Bildung und Forschung (Federal Ministry for Education and Research) [grant number 02NUK073 (TOGETHER)], M.R. is funded by the Bavarian Research Foundation (MikroHyperTumImmun, grant number AZ-1495-20, Bayerische Forschungsstiftung). C.L. and A.R. are further supported by the Deutsche Forschungsgemeinschaft (DFG, German Research Foundation) – project number 391977956 – SFB 1357.

Acknowledgments

We would like to thank Andrea Eichhorn, Elke Kretzschmar, and Jörg Pekarsky (all Institute of Anatomy, FAU Erlangen-Nürnberg, Erlangen, Germany) as well as Dr. Benjamin Frey (Department of Radiation Oncology, FAU Erlangen-Nürnberg, Erlangen, Germany), Dr. Anja Beckmann and Alexander Grissmer (both Institute of Anatomy, Saarland University, Homburg/Saar, Germany) for their excellent technical assistance, Valentina Jüngert for English proofreading as well as Leon Hierhammer for his assistance in graphic design. We acknowledge support by Deutsche Forschungsgemeinschaft (DFG) and Friedrich-Alexander-Universität Erlangen-Nürnberg (FAU) within the funding program Open Access Publishing.

Author's note

The present work was performed in (partial) fulfilment of the requirements for obtaining the degree „Dr. med." at the Medical Faculty of the Friedrich-Alexander-Universität Erlangen-Nürnberg (FAU).

References

1. Jiang B, Kauffman AE, Li L, McFee W, Cai B, Weinstein J et al. Health impacts of environmental contamination of micro- and nanoplastics: a review. Environ Health Prev Med 2020; 25(1):29. doi: 10.1186/s12199-020-00870-9.

2. Ramsperger AFRM, Bergamaschi E, Panizzolo M, Fenoglio I, Barbero F, Peters R et al. Nano- and microplastics: a comprehensive review on their exposure routes, translocation, and fate in humans. NanoImpact 2023; 29:100441. doi: 10.1016/j.impact.2022.100441.

3. Wang X, Ren X-M, He H, Li F, Liu K, Zhao F et al. Cytotoxicity and pro-inflammatory effect of polystyrene nano-plastic and micro-plastic on RAW264.7 cells. Toxicology 2023; 484:153391. doi: 10.1016/j.tox.2022.153391.

4. Koner S, Florance I, Mukherjee A, Chandrasekaran N. Cellular response of THP-1 macrophages to polystyrene microplastics exposure. Toxicology 2023; 483:153385. doi: 10.1016/j.tox.2022.153385.

5. Wright SL, Thompson RC, Galloway TS. The physical impacts of microplastics on marine organisms: a review. Environ Pollut 2013; 178:483–92. doi: 10.1016/j.envpol.2013.02.031.

6. Liu K, Wang X, Fang T, Xu P, Zhu L, Li D. Source and potential risk assessment of suspended atmospheric microplastics in Shanghai. Sci Total Environ 2019; 675:462–71. doi: 10.1016/j.scitotenv.2019.04.110.

7. Kernchen S, Löder MGJ, Fischer F, Fischer D, Moses SR, Georgi C et al. Airborne microplastic concentrations and deposition across the Weser River catchment. Sci Total Environ 2022; 818:151812. doi: 10.1016/j.scitotenv.2021.151812.

8. Yang L, Zhang Y, Kang S, Wang Z, Wu C. Microplastics in soil: A review on methods, occurrence, sources, and potential risk. Sci Total Environ 2021; 780:146546. doi: 10.1016/j.scitotenv.2021.146546.

9. Deng Y, Zhang Y, Lemos B, Ren H. Tissue accumulation of microplastics in mice and biomarker responses suggest widespread health risks of exposure. Sci Rep 2017; 7:46687. doi: 10.1038/srep46687.

10. Jin Y, Lu L, Tu W, Luo T, Fu Z. Impacts of polystyrene microplastic on the gut barrier, microbiota and metabolism of mice. Sci Total Environ 2019; 649:308–17. doi: 10.1016/j.scitotenv.2018.08.353.

11. Yee MS-L, Hii L-W, Looi CK, Lim W-M, Wong S-F, Kok Y-Y et al. Impact of Microplastics and Nanoplastics on Human Health. Nanomaterials (Basel) 2021; 11(2). doi: 10.3390/nano11020496.

12. Leslie HA, van Velzen MJM, Brandsma SH, Vethaak AD, Garcia-Vallejo JJ, Lamoree MH. Discovery and quantification of plastic particle pollution in human blood. Environ Int 2022; 163:107199. doi: 10.1016/j.envint.2022.107199.

13. Kontou S, Dessipri E, Lampi E. Determination of styrene monomer migrating in foodstuffs from polystyrene food contact articles using HS-SPME-GC-MS/MS: Results from the Greek market. Food Addit Contam Part A Chem Anal Control Expo Risk Assess 2022; 39(2):415–27. doi: 10.1080/19440049.2021.2005830.

14. Shi Q, Tang J, Wang L, Liu R, Giesy JP. Combined cytotoxicity of polystyrene nanoplastics and phthalate esters on human lung epithelial A549 cells and its mechanism. Ecotoxicol Environ Saf 2021; 213:112041. doi: 10.1016/j.ecoenv.2021.112041.

15. Blackburn K, Green D. The potential effects of microplastics on human health: What is known and what is unknown. Ambio 2022; 51(3):518–30. doi: 10.1007/s13280-021-01589-9.

16. Murphy K, Weaver C. Das mucosale Immunsystem. In: Murphy, Hrsg. Janeway Immunologie. Berlin, Heidelberg: Springer Berlin Heidelberg; 2018. S. 641–91.

17. Di Tommaso N, Gasbarrini A, Ponziani FR. Intestinal Barrier in Human Health and Disease. Int J Environ Res Public Health 2021; 18(23). doi: 10.3390/ijerph182312836.

18. Weibel ER. Lung morphometry: the link between structure and function. Cell Tissue Res 2017; 367(3):413–26. doi: 10.1007/s00441-016-2541-4.

19. Nguyen AV, Soulika AM. The Dynamics of the Skin's Immune System. Int J Mol Sci 2019; 20(8). doi: 10.3390/ijms20081811.

20. Uribe-Querol E, Rosales C. Phagocytosis: Our Current Understanding of a Universal Biological Process. Front Immunol 2020; 11:1066. doi: 10.3389/fimmu.2020.01066.

21. Jeon S, Lee D-K, Jeong J, Yang SI, Kim J-S, Kim J et al. The reactive oxygen species as pathogenic factors of fragmented microplastics to macrophages. Environ Pollut 2021; 281:117006. Verfügbar unter: https://pubmed.ncbi.nlm.nih.gov/33812130/.

22. Chanput W, Mes JJ, Wichers HJ. THP-1 cell line: an in vitro cell model for immune modulation approach. Int Immunopharmacol 2014; 23(1):37–45. doi: 10.1016/j.intimp.2014.08.002.

23. Gstraunthaler G, Lindl T. Zell- und Gewebekultur: Allgemeine Grundlagen und spezielle Anwendungen. 8. Auflage. Berlin: Springer Spektrum; 2021.

24. Collin-Faure V, Vitipon M, Torres A, Tanyeres O, Dalzon B, Rabilloud T. The internal dose makes the poison: higher internalization of polystyrene particles induce increased perturbation of macrophages. Front Immunol 2023; 14:1092743. doi: 10.3389/fimmu.2023.1092743.

25. Merkley SD, Moss HC, Goodfellow SM, Ling CL, Meyer-Hagen JL, Weaver J et al. Polystyrene microplastics induce an immunometabolic active state in macrophages. Cell Biol Toxicol 2022; 38(1):31–41. doi: 10.1007/s10565-021-09616-x.

26. Tavakolpournegari A, Annangi B, Villacorta A, Banaei G, Martin J, Pastor S et al. Hazard assessment of different-sized polystyrene nanoplastics in hematopoietic human cell lines. Chemosphere 2023; 325:138360. doi: 10.1016/j.chemosphere.2023.138360.

27. Hirayama D, Iida T, Nakase H. The Phagocytic Function of Macrophage-Enforcing Innate Immunity and Tissue Homeostasis. Int J Mol Sci 2017; 19(1). doi: 10.3390/ijms19010092.

28. Shapouri-Moghaddam A, Mohammadian S, Vazini H, Taghadosi M, Esmaeili S-A, Mardani F et al. Macrophage plasticity, polarization, and function in health and disease. J Cell Physiol 2018; 233(9):6425–40. doi: 10.1002/jcp.26429.

29. Wedekind H, Walz K, Buchbender M, Rieckmann T, Strasser E, Grottker F et al. Head and neck tumor cells treated with hypofractionated irradiation die via apoptosis and are better taken up by M1-like macrophages. Strahlenther Onkol 2022; 198(2):171–82. doi: 10.1007/s00066-021-01856-4.

30. Duits DEM, Wellenstein MD, Visser KE de. In vitro assessment of cancer cell-induced polarization of macrophages. Methods Enzymol 2020; 632:133–54. doi: 10.1016/bs.mie.2019.06.011.

31. Hampel U, Garreis F, Burgemeister F, Eßel N, Paulsen F. Effect of intermittent shear stress on corneal epithelial cells using an in vitro flow culture model. Ocul Surf 2018; 16(3):341–51. doi: 10.1016/j.jtos.2018.04.005.

32. Vieira-da-Silva B, Castanho MARB. Resazurin Reduction-Based Assays Revisited: Guidelines for Accurate Reporting of Relative Differences on Metabolic Status. Molecules 2023; 28(5). doi: 10.3390/molecules28052283.

33. Kumar P, Nagarajan A, Uchil PD. Analysis of Cell Viability by the Lactate Dehydrogenase Assay. Cold Spring Harb Protoc 2018; 2018(6). doi: 10.1101/pdb.prot095497.

34. Crowley LC, Marfell BJ, Scott AP, Waterhouse NJ. Quantitation of Apoptosis and Necrosis by Annexin V Binding, Propidium Iodide Uptake, and Flow Cytometry. Cold Spring Harb Protoc 2016; 2016(11). doi: 10.1101/pdb.prot087288.

35. Cutolo M, Campitiello R, Gotelli E, Soldano S. The Role of M1/M2 Macrophage Polarization in Rheumatoid Arthritis Synovitis. Front Immunol 2022; 13:867260. doi: 10.3389/fimmu.2022.867260.

36. Ball MS, Shipman EP, Kim H, Liby KT, Pioli PA. CDDO-Me Redirects Activation of Breast Tumor Associated Macrophages. PLoS One 2016; 11(2):e0149600. doi: 10.1371/journal.pone.0149600.

37. Wang X, Roper MG. Measurement of DCF fluorescence as a measure of reactive oxygen species in murine islets of Langerhans. Anal Methods 2014; 6(9):3019–24. doi: 10.1039/C4AY00288A.

38. Murphy MP, Bayir H, Belousov V, Chang CJ, Davies KJA, Davies MJ et al. Guidelines for measuring reactive oxygen species and oxidative damage in cells and in vivo. Nat Metab 2022; 4(6):651–62. doi: 10.1038/s42255-022-00591-z.

39. Brüne B, Dehne N, Grossmann N, Jung M, Namgaladze D, Schmid T et al. Redox control of inflammation in macrophages. Antioxid Redox Signal 2013; 19(6):595–637. doi: 10.1089/ars.2012.4785.

40. Corbett Y, D'Alessandro S, Parapini S, Scaccabarozzi D, Kalantari P, Zava S et al. Interplay between Plasmodium falciparum haemozoin and L-arginine: implication for nitric oxide production. Malar J 2018; 17(1):456. doi: 10.1186/s12936-018-2602-0.

41. Stock V, Böhmert L, Lisicki E, Block R, Cara-Carmona J, Pack LK et al. Uptake and effects of orally ingested polystyrene microplastic particles in vitro and in vivo. Arch Toxicol 2019; 93(7):1817–33. doi: 10.1007/s00204-019-02478-7.

42. Li L, Sun S, Tan L, Wang Y, Wang L, Zhang Z et al. Polystyrene Nanoparticles Reduced ROS and Inhibited Ferroptosis by Triggering Lysosome Stress and TFEB Nucleus Translocation in a Size-Dependent Manner. Nano Lett 2019; 19(11):7781–92. doi: 10.1021/acs.nanolett.9b02795.

43. Ramsperger AFRM, Narayana VKB, Gross W, Mohanraj J, Thelakkat M, Greiner A et al. Environmental exposure enhances the internalization of microplastic particles into cells. Sci Adv 2020; 6(50). doi: 10.1126/sciadv.abd1211.

44. Malafaia G, Da Luz TM, Ahmed MAI, Karthi S, Da Araújo APC. When toxicity of plastic particles comes from their fluorescent dye: a preliminary study involving neotropical Physalaemus cuvieri tadpoles and polyethylene microplastics. Journal of Hazardous Materials Advances 2022; 6:100054. Verfügbar unter: https://www.sciencedirect.com/science/article/pii/S2772416622000110.

45. Schür C, Rist S, Baun A, Mayer P, Hartmann NB, Wagner M. When Fluorescence Is not a Particle: The Tissue Translocation of Microplastics in Daphnia magna Seems an Artifact. Environ Toxicol Chem 2019; 38(7):1495–503. doi: 10.1002/etc.4436.

46. Paget V, Dekali S, Kortulewski T, Grall R, Gamez C, Blazy K et al. Specific uptake and genotoxicity induced by polystyrene nanobeads with distinct surface chemistry on human lung epithelial cells and macrophages. PLoS One 2015; 10(4):e0123297. doi: 10.1371/journal.pone.0123297.

47. Wieland S, Ramsperger AFRM, Gross W, Lehmann M, Witzmann T, Caspari A et al. Nominally identical microplastic models differ greatly in their particle-cell interactions. Nat Commun 2024; 15(1):922. doi: 10.1038/s41467-024-45281-4.

48. Ramsperger AFRM, Jasinski J, Völkl M, Witzmann T, Meinhart M, Jérôme V et al. Supposedly identical microplastic particles substantially differ in their material properties influencing particle-cell interactions and cellular responses. J Hazard Mater 2022; 425:127961. doi: 10.1016/j.jhazmat.2021.127961.

49. Jasinski J, Völkl M, Hahn J, Jérôme V, Freitag R, Scheibel T. Polystyrene microparticle distribution after ingestion by murine macrophages. J Hazard Mater 2023; 457:131796. doi: 10.1016/j.jhazmat.2023.131796.

50. Busch M, Bredeck G, Waag F, Rahimi K, Ramachandran H, Bessel T et al. Assessing the NLRP3 Inflammasome Activating Potential of a Large Panel of Micro- and Nanoplastics in THP-1 Cells. Biomolecules 2022; 12(8). doi: 10.3390/biom12081095.

51. Prietl B, Meindl C, Roblegg E, Pieber TR, Lanzer G, Fröhlich E. Nano-sized and micro-sized polystyrene particles affect phagocyte function. Cell Biol Toxicol 2014; 30(1):1–16. doi: 10.1007/s10565-013-9265-y.

52. Wolff CM, Singer D, Schmidt A, Bekeschus S. Immune and inflammatory responses of human macrophages, dendritic cells, and T-cells in presence of micro- and nanoplastic of different types and sizes. J Hazard Mater 2023; 459:132194. doi: 10.1016/j.jhazmat.2023.132194.

53. Wang X, Zhang X, Sun K, Wang S, Gong D. Polystyrene microplastics induce apoptosis and necroptosis in swine testis cells via ROS/MAPK/HIF1α pathway. Environ Toxicol 2022; 37(10):2483–92. doi: 10.1002/tox.23611.

54. Zhang Q, Wang F, Xu S, Cui J, Li K, Shiwen X et al. Polystyrene microplastics induce myocardial inflammation and cell death via the TLR4/NF-κB pathway in carp. Fish Shellfish Immunol 2023; 135:108690. doi: 10.1016/j.fsi.2023.108690.

55. Shi X, Wang X, Huang R, Tang C, Hu C, Ning P et al. Cytotoxicity and Genotoxicity of Polystyrene Micro- and Nanoplastics with Different Size and Surface Modification in A549 Cells. Int J Nanomedicine 2022; 17:4509–23. doi: 10.2147/IJN.S381776.

56. Das A. The emerging role of microplastics in systemic toxicity: Involvement of reactive oxygen species (ROS). Sci Total Environ 2023; 895:165076. doi: 10.1016/j.scitotenv.2023.165076.

57. Herb M, Schramm M. Functions of ROS in Macrophages and Antimicrobial Immunity. Antioxidants (Basel) 2021; 10(2). doi: 10.3390/antiox10020313.

58. Berlett BS, Stadtman ER. Protein oxidation in aging, disease, and oxidative stress. J Biol Chem 1997; 272(33):20313–6. doi: 10.1074/jbc.272.33.20313.

59. Griffiths HR, Dias IHK, Willetts RS, Devitt A. Redox regulation of protein damage in plasma. Redox Biol 2014; 2:430–5. doi: 10.1016/j.redox.2014.01.010.

60. Rubio L, Barguilla I, Domenech J, Marcos R, Hernández A. Biological effects, including oxidative stress and genotoxic damage, of polystyrene nanoparticles in different human hematopoietic cell lines. J Hazard Mater 2020; 398:122900. doi: 10.1016/j.jhazmat.2020.122900.

61. Lunov O, Syrovets T, Loos C, Nienhaus GU, Mailänder V, Landfester K et al. Amino-functionalized polystyrene nanoparticles activate the NLRP3 inflammasome in human macrophages. ACS Nano 2011; 5(12):9648–57. doi: 10.1021/nn203596e.

62. Robbins RA, Grisham MB. Nitric oxide. Int J Biochem Cell Biol 1997; 29(6):857–60. doi: 10.1016/s1357-2725(96)00167-7.

63. Ueki Y, Miyake S, Tominaga Y, Eguchi K. Increased nitric oxide levels in patients with rheumatoid arthritis. J Rheumatol 1996; 23(2):230–6.

64. Wanchu A, Khullar M, Deodhar SD, Bambery P, Sud A. Nitric oxide synthesis is increased in patients with systemic lupus erythematosus. Rheumatol Int 1998; 18(2):41–3. doi: 10.1007/s002960050055.

65. Bagasra O, Michaels FH, Zheng YM, Bobroski LE, Spitsin SV, Fu ZF et al. Activation of the inducible form of nitric oxide synthase in the brains of patients with multiple sclerosis. Proc Natl Acad Sci U S A 1995; 92(26):12041–5. doi: 10.1073/pnas.92.26.12041.

66. Palmieri EM, McGinity C, Wink DA, McVicar DW. Nitric Oxide in Macrophage Immunometabolism: Hiding in Plain Sight. Metabolites 2020; 10(11). doi: 10.3390/metabo10110429.

67. Beltrán B, Mathur A, Duchen MR, Erusalimsky JD, Moncada S. The effect of nitric oxide on cell respiration: A key to understanding its role in cell survival or death. Proc Natl Acad Sci U S A 2000; 97(26):14602–7. doi: 10.1073/pnas.97.26.14602.

68. Labonte AC, Tosello-Trampont A-C, Hahn YS. The role of macrophage polarization in infectious and inflammatory diseases. Mol Cells 2014; 37(4):275–85. doi: 10.14348/molcells.2014.2374.

69. Almradi A, Hanzel J, Sedano R, Parker CE, Feagan BG, Ma C et al. Clinical Trials of IL-12/IL-23 Inhibitors in Inflammatory Bowel Disease. BioDrugs 2020; 34(6):713–21. doi: 10.1007/s40259-020-00451-w.

70. Murray PJ, Wynn TA. Protective and pathogenic functions of macrophage subsets. Nat Rev Immunol 2011; 11(11):723–37. doi: 10.1038/nri3073.

71. Bertani FR, Mozetic P, Fioramonti M, Iuliani M, Ribelli G, Pantano F et al. Classification of M1/M2-polarized human macrophages by label-free hyperspectral reflectance confocal microscopy and multivariate analysis. Sci Rep 2017; 7(1):8965. doi: 10.1038/s41598-017-08121-8.

72. Fuchs A-K, Syrovets T, Haas KA, Loos C, Musyanovych A, Mailänder V et al. Carboxyl- and amino-functionalized polystyrene nanoparticles differentially affect the polarization profile of M1 and M2 macrophage subsets. Biomaterials 2016; 85:78–87. doi: 10.1016/j.biomaterials.2016.01.064.

73. Koning N, van Eijk M, Pouwels W, Brouwer MSM, Voehringer D, Huitinga I et al. Expression of the inhibitory CD200 receptor is associated with alternative macrophage activation. J Innate Immun 2010; 2(2):195–200. doi: 10.1159/000252803.

74. Vogel DYS, Glim JE, Stavenuiter AWD, Breur M, Heijnen P, Amor S et al. Human macrophage polarization in vitro: maturation and activation methods compared. Immunobiology 2014; 219(9):695–703. doi: 10.1016/j.imbio.2014.05.002.

75. Xiao B, Liu Y, Chandrasiri I, Overby C, Benoit DSW. Impact of Nanoparticle Physicochemical Properties on Protein Corona and Macrophage Polarization. ACS Appl Mater Interfaces 2023. doi: 10.1021/acsami.2c22471.

Declaration of interests

☒ The authors declare that they have no known competing financial interests or personal relationships that could have appeared to influence the work reported in this paper.

Highlights

- Human monocyte-derived macrophages as novel *in vitro* model to study effects of MNP
- Concentration-dependent cytoplasmic uptake of PS MNBs visualized by TEM and SEM
- Uptake of PS MNBs by primary human macrophages is visible in live cell imaging
- Effects of different sized, non-fluorescent PS-MNBs in physiological concentration
- PS MNBs induce nitric oxide formation and cytotoxic effects in human macrophages